

2021-01-11

PETROLOGY AND GEOCHEMISTRY OF VOLCANIC ROCKS AND ASSOCIATED MAFIC DYKES IN THE BIRSHELEKO AREA, NORTHWESTERN ETHIOPIAN PLATEAU

KIDIST TESFA

<http://ir.bdu.edu.et/handle/123456789/11845>

Downloaded from DSpace Repository, DSpace Institution's institutional repository



BAHIR DAR UNIVERSITY
GRADUATE STUDIE OFFICE
SCHOOL OF EARTH SCIENCES

**PETROLOGY AND GEOCHEMISTRY OF VOLCANIC
ROCKS AND ASSOCIATED MAFIC DYKES IN THE
BIRSHELEKO AREA, NORTHWESTERN ETHIOPIAN
PLATEAU**

BY
KIDIST TESFA ZEGEYE

OCTOBER, 2020

BAHIR DAR UNIVERSITY

School of Earth Sciences

Department of Geology

**PETROLOGY AND GEOCHEMISTRY OF VOLCANIC
ROCKS AND ASSOCIATED MAFIC DYKES IN THE
BIRSHELEKO AREA, NORTHWESTERN ETHIOPIAN
PLATEAU**

A THESIS SUBMITTED TO SCHOOL OF EARTH SCIENCES, BAHIR DAR
UNIVERSITY, IN PARTIAL FULFILLMENT OF THE REQUIREMENTS FOR THE
DEGREE MASTERS OF SCIENCE IN PETROLOGY

BY

KIDIST TESFA ZEGEYE

ADVISOR: MINYAHL TEFERI DESTA (PhD)

OCTOBER, 2020

BAHIRDAR, ETHIOPIA

BAHIR DAR UNIVERSITY
SCHOOL OF EARTH SCIENCES
DEPARTMENT OF GEOLOGY
Approval of Thesis for defense

I hereby certify that I have supervised, read, and evaluated this thesis titled “petrology and geochemistry of volcanic rocks and associated mafic dykes in the Birsheleko area, northwestern Ethiopian plateau” by kidist Tesfa prepared under my guidance. I recommend the Thesis to be submitted for the oral defense.

_____	_____	_____
Advisor’s name	Date	Signature

BAHIR DAR UNIVERSITY
SCHOOL OF EARTH SCIENCES
DEPARTMENT OF GEOLOGY

**Petrology and geochemistry of volcanic rocks and associated mafic dykes
in the Birsheleko area, northwestern Ethiopian plateau**

Approval of the thesis for defense result

We hereby certify that we have examined this thesis entitled “petrology and geochemistry of volcanic rocks and associated mafic dykes in the Birsheleko area, northwestern Ethiopian plateau” by Kidist Tesfa, We recommend that the thesis is approved for the degree of “Masters in petrology”.

Board of Examiners

_____	_____	_____
External examiner’s name	Signature	Date
_____	_____	_____
Internal examiner’s name	Signature	Date
_____	_____	_____
Chair person’s name	Signature	Date

Declaration of Originality

I hereby declare that this thesis is my original master's degree entitled "Petrology and geochemistry of volcanic rocks and associated mafic dykes in the Birsheleko area, northwestern Ethiopian plateau" was prepared by me, with the supervision of Dr. Minyahl Teferi, school of Earth Science, Bahir Dar University during the year 2019/2020. This thesis is my original work and has not been presented for a degree qualification in any other university, and all sources of materials used for the thesis have been duly acknowledged.

Kidist Tesfa

Candidate

Signature

Date

ACKNOWLEDGMENT

I would like to express my deepest gratitude to my advisor Dr. Minyahl Teferi for his consistent advice, guidance, and his ultimate help at the various stage of this thesis work starting from the beginning to the end. I am grateful to Bahir Dar University for sponsoring my study and giving me an invaluable opportunity to study for a master's degree. My great thanks also go to Bahir Dar university school of earth sciences staff members. Specially to Mohammed Seid mohammedyasin, Ayenachew Alemayehu, Alebachew Tarekegn, and Tesfaye Chala for their help. I am also thankful to Dr. Daniel Meshesha for his constructive comments during proposal preparation.

My profound gratitude goes to my friends Mulugeta Tadele, Endalkachew Abebaw, and Yoseph Muhabaw, for their support in the field data collection. Immeasurable thanks go to my father Tesfa Zegeye, my mother Asefash Tegegne, my brothers Andualem Tesfa, and Ermiyas Tesfa. I have no words to appreciate their roles in my life, simply thank you. Love you a lot.

ABSTRACT

This study is conducted in the Birsheleko area, NW Ethiopian plateau. The main aim is to determine the Petrogenesis of volcanic rocks and associated mafic dykes. To accomplish the research objective field investigation, petrographic and major and trace element geochemical analysis using a combination of ICP-MS and ICP-AES methods was applied. The lithological units identified in the study area are basalt, scoria cones, dolerite, and basaltic andesite. Basaltic andesite and dolerite are exposed as a dyke, besides; basaltic units cover most of the study area. The studied samples are characterized by aphyric to porphyritic texture with a variable proportion of plagioclase, olivine, and pyroxene as phenocryst. The groundmass is composed of plagioclase, olivine iron-titanium oxides (opaque minerals), clinopyroxene, and orthopyroxene. Based on the modal analysis the rocks are divided into pyroxene phyric basalt, Olivine phyric basalt, plagioclase phyric basalt, plagioclase phyric dolerite, and aphyric trachy flow basalt and basaltic andesite.

Most of the studied samples fall into the tholeiitic group, however; two samples were grouped into transitional and alkaline groups. From the Harker variation diagram, most of the major and trace elements did not show a clear trend instead they are scattered suggesting the compositional variation of the studied rocks cannot be explained in terms of fractional crystallization. In the primitive mantle normalized multi-element diagram the tholeiitic samples show depletions in Rb, Th, Ce, Pr, P, and Nb and prominent peaks at Ba, K, Pb, U, and Sr. However, the transitional and alkaline basaltic rocks show enrichment in Pb, Sr, Nb, Ba, depletion in Sm, Pr, without and the positive anomaly at U and K. This indicates that the tholeiites might experienced crustal contamination and the alkaline and transitional basalts are not. From $(Gd/Sm)_N$ vs. $(La/Sm)_N$ diagram, it is determined that all the studied tholeiitic samples are formed by the melting of the spinel peridotite mantle source at a high degree of partial melting and shallow depth. In the contrast, the transitional and alkaline basalts are formed by the melting of the garnet peridotite mantle source by a low degree of partial melting at a greater depth than the tholeiites.

Keywords: Crustal contamination, Degree of partial melting, Geochemistry, Northwestern Ethiopian plateau, Petrography.

TABLE OF CONTENTS

Contents	Pages
Declaration of Originality	i
ACKNOWLEDGMENT.....	ii
ABSTRACT.....	iii
LIST OF FIGURES	vii
LIST OF TABLES.....	ix
LIST OF ACRONYMS	x
CHAPTER ONE.....	1
1 INTRODUCTION	1
1.2 Geographic setting of the Study Area.....	2
1.2.1 Location and accessibility.....	2
1.2.2 Physiography.....	3
1.2.3 Climate condition.....	4
1.3 Objectives	6
1.3.1 General objective.....	6
1.3.2 Specific objectives.....	6
1.4 Statement of the problem and research questions	6
1.5 Methodology.....	7
1.5.1 Field investigation.....	7
1.5.2 Data analysis and organization.....	7
1.5.2.1 Petrographic analysis.....	7
1.5.2.2 Geochemical analysis.....	8
1.6 Expected outcome and significance of the research.....	9
CHAPTER TWO	10
2. REGIONAL GEOLOGIC SETTING.....	10
2.1 The Ethiopian continental flood basalt.....	10
2.2 Volcanics of Northwestern Ethiopian plateau	11

CHAPTER THREE	14
3. GEOLOGY OF THE STUDY AREA	14
3.1 Lithological description.....	14
3.1.1 Basalt.....	14
3.1.2 Basaltic Andesite.....	15
3.1.3 Dolerite.....	15
3.1.4 Scoria cones.....	16
3.2 Petrography.....	17
3.2.1 Plagioclase phyric basalt and dolerite.....	17
3.2.2 Pyroxene phyric basalt.....	19
3.2.3 Olivine phyric basalts.....	21
3.2.4 Aphyric-trachy flow basalt and basaltic andesite.....	22
3.3 Geological structures	25
3.3.1 Joint.....	25
3.3.2 Fault.....	25
CHAPTER FOUR.....	27
4. WHOLE ROCK GEOCHEMISTRY	27
4.1 Introduction	27
4.2 Major elements geochemistry and rock classification.....	34
4.3 Trace element geochemistry.....	36
4.4 Rare earth element pattern.....	38
CHAPTER FIVE	42
5. DISCUSSION.....	42
5.1 Fractional crystallization	42
5.2 Interaction with crustal materials	43
5.3 Mantle source characteristics.....	44
5.4 Degree of partial melting.....	45
5.5 Comparison of the Birsheleko area basaltic rocks with the Ethiopian continental flood basalts	46

CHAPTER SIX.....	51
6. CONCLUSION AND RECOMMENDATION.....	51
6.1 Conclusion.....	51
6.2 Recommendation.....	52
References.....	53
Appendix.....	59

LIST OF FIGURES

Figure 1.1: Location and accessibility map of the study area.	3
Figure 1.2: Physiographic map of the Birsheleko area.	4
Figure 1.3: A bar chart that shows a mean monthly temperature of the Birsheleko area.....	5
Figure 1.4: A bar chart that shows a mean monthly Rainfall of the Birsheleko area	5
Figure 2.1: Geological map of the central and Northwestern Ethiopian plateau showing the extent of the flood volcanism (Adopted from Kieffer et al., 2004).	13
Figure 3.1: a) Amygdaloidal basaltic rock units exposed by a river b) Vesicular basalt.	15
Figure 3.2: Field photograph of Basaltic andesite which is exposed as dyke around Gedame Iyesus church.	15
Figure 3.3: Field photograph of a) exfoliation b) dolerite.	16
Figure 3.4: A) Field photograph showing a half breached morphology of Pyroclasts. B) Volcanic bomb	17
Figure 3.5: Thin section photomicrographs of the plagioclase phyric basalt and dolerite rock units.....	18
Figure 3.6: Thin section photomicrographs of the pyroxene phyric basalt rock	20
Figure 3.7: Thin section photomicrographs of the Olivine phyric basalts.....	22
Figure 3.8: Microphotographs of a) Aphyric trachy flow basalt under XPL (sample BS-2). B) aphyric trachytic basaltic andesite.	23
Figure 3.9 : a) Geological map of the study area at a scale of 1:50,000 b) Cross-sectional profile with normal fault.....	24
Figure 3.10: Field photograph of joints a columnar joint on highly weathered basalt exposed by Inbodbod River.	26
Figure 3.11: a) Rose diagram Strike of the joints. b) Equal angel plot of joints in the form of a pole.....	26
Figure 4.1: Selected trace elements vs. Zr and Th diagrams for checking element mobility during post-eruption.....	29
Figure 4.2: a) Total alkali vs. silica diagram (after Le Bas et al., 1986), for the classification of volcanic rocks of the Birsheleko volcanic rocks b) AFM diagram for volcanic rocks of Birsheleko from Irvine and Baragars (1971).	35
Figure 4.3: Variation diagram for major oxides against MgO.....	36

Figure 4.4: Variation diagram of compatible trace elements vs. MgO.....	37
Figure 4.5: Variation diagram of incompatible trace elements versus MgO (wt. %),.....	38
Figure 4.6: Chondrite normalized REE spider diagram of rocks.....	39
Figure 4.7: Primitive mantle normalized multi-element diagram	40
Figure 4.8: Nb Vs. Zr plots to determine the genetic relationship between the tholeiitic, transitional, and alkaline after (Hutchison et al., 2016).....	41
Figure 5.1:(La /Sm) _N vs. (Gd /Yb) _N for Birsheleko volcanic rocks and associated mafic dykes to determine mantle source after (Alvaro et al., 2014)	46.
Figure 5.2: Nb/ Y versus Ti/ Y diagram for Birsheleko area volcanic rocks and associated mafic dykes after (Pik et al., 1998).....	48
Figure 5.3: Ce/Pb vs. MgO (wt. %) after Hofmann et al. (1986) for the Birsheleko volcanic rocks and associated mafic dykes	49

LIST OF TABLES

Table 4.1 Major oxide concentration in (wt. %) for representative samples from the Birsheleko area volcanic rocks and associated mafic dykes.....	30
Table 4.2 Trace elements concentration in (ppm) for representative samples from the Birsheleko area volcanic rocks and associated mafic dykes.....	31
Table 4.3 CIPW norm calculations in (wt. %) for the Birsheleko volcanic rocks.....	33

LIST OF ACRONYMS

4X	Four times magnification
CFB	Continental Flood Basalt
CIPW	Cross Idings Pirsson and Washington
DEM	Digital Elevation Model
E-MORB	Enriched MORB
GSE	Geological Survey of Ethiopia
HFSE	High Field Strength Elements
HIMU	High- μ , mantle (Pb enriched)
HREE	Heavy rare earth element
HT1	first high-Titanium basalt
HT2	second high-Titanium basalt
ICP-AES	Inductively Coupled Plasma Atomic Emission Spectroscopy
ICP-MS	Inductively Coupled Plasma Mass Spectrometry
LILE	Large Ion Lithophile Elements
LOI	Loss on ignition
LREE	Light Rare Earth Element
LT	Low-Titanium basalt
M.S.L	Mean average sea level
Ma	Million years ago
MER	Main Ethiopian Rift

MORB	Mid-ocean ridge basalt
Mt	Mountain
N-MORB	Normal MORB
OIB	Ocean island basalt
PPL	Plane polarized light
ppm	Parts per million
REE	Rare Earth Element
SEP	Southern Ethiopian Plateau
TAS	Total alkali-silica
WEP	Western Ethiopian Plateau
Wt %	Weight percentage
XPL	Cross polarized light

CHAPTER ONE

1. 1 INTRODUCTION

Petrological and geochemical data of igneous rocks are useful to determine and interpret source composition, fractional crystallization, effects of crustal contamination, processes involved in the melting, and the emplacement or tectonic environment of the rocks (Best, 2003; Singh, 2012; Winter, 2014). Generally, they are important to determine the origin of rocks i.e. Petrogenesis, which is the main objective of this study. The present study is conducted in the Birsheleko area, Northwestern Ethiopian plateau, that is the area in which Oligocene (pre-rift) volcanic rocks that formed as a result of Afro Arabian separation are found overlain by large central vent erupted Miocene volcanoes (Mohr and Zanettin, 1988; Pik et al ., 1998).

The volcanic province of Ethiopia consists of spatially distributed low titanium to High titanium and ultra-high titanium basalts and picrites (Pik et al. ,1998 and Desta et al .,2014). In which the magma was produced by melting the mantle at different pressure and temperature conditions (Kieffer et al., 2004 and Beccaluva et al.,2009). It is overlain by alkaline basalts that have xenoliths i.e. direct mantle sources and shield volcanoes. The most common shield centers are Semien (30 Ma), Choke (22.4 Ma), Gugufu (22.3 Ma), and Guna (10.7 Ma) mountains (Kieffer et al., 2004) estimated total areal coverage, which accounted for 20 % of the surface of the plateau Besides, The triple junction of Afar is also found in the Ethiopian volcanic province suggested being a source of the deep mantle plume. The occurrence of those above things makes the region more attractive for geologists (Pik et al.,1998; Pik et al .,1999; Kieffer et al., 2004; Beccaluva et al., 2009; Desta et al., 2014). As a result, most studies have been done in the province (e.g., Mohr and Zanettin,1988; Ayalew and Yirgu, 2003; Kieffer et al., 2004; Ayalew et al., 2016; Hagos et al., 2016). However, locally detailed investigations on any particular single section of the plateau are scarce. The petrology and geochemistry of the Birsheleko area were done as a part of the Bure area volcanic rocks by Meshesha and Shinjo (2004, 2007) with a limited number of samples regionally. However, there were no enough representative samples taken from the Birsheleko

area. Therefore, the new petrologic and geochemical data from Birsheleko volcanic rocks can potentially provide additional constraints regarding the characteristics of the magma sources. So, this study is done using petrographic, major, and trace element data to investigate the petrology and geochemistry, the possible source of the volcanic rocks and associated mafic dykes from the Birsheleko area. Besides, to compare and contrast the result with the previous works done in the Northwestern Ethiopian plateau and Main Ethiopian Rift.

1.2 Geographic setting of the Study Area

1.2.1 Location and accessibility

This research is conducted in the Birsheleko area in Northwestern Ethiopia (Fig.1.1). The area lies on the Bure and Kuch Sub-sheet with sheet number **1037A3** and **1037C1** according to the topographic map distribution of the Ethiopian Mapping Agency (EMA). It can be easily accessed through main asphalt roads which run from Bahir Dar-Merawi-Durbete-Dangla Injibara, Bure, Mankusa, and then reach Birsheleko. Besides, it can be accessed through the road from Addis Ababa (the capital city of Ethiopia) via Debre Markos to Biresheleko. Geographically the study area is bounded by a grid of Easting from 281885m to 304507m and northing of 1149486 m to 1183876m.

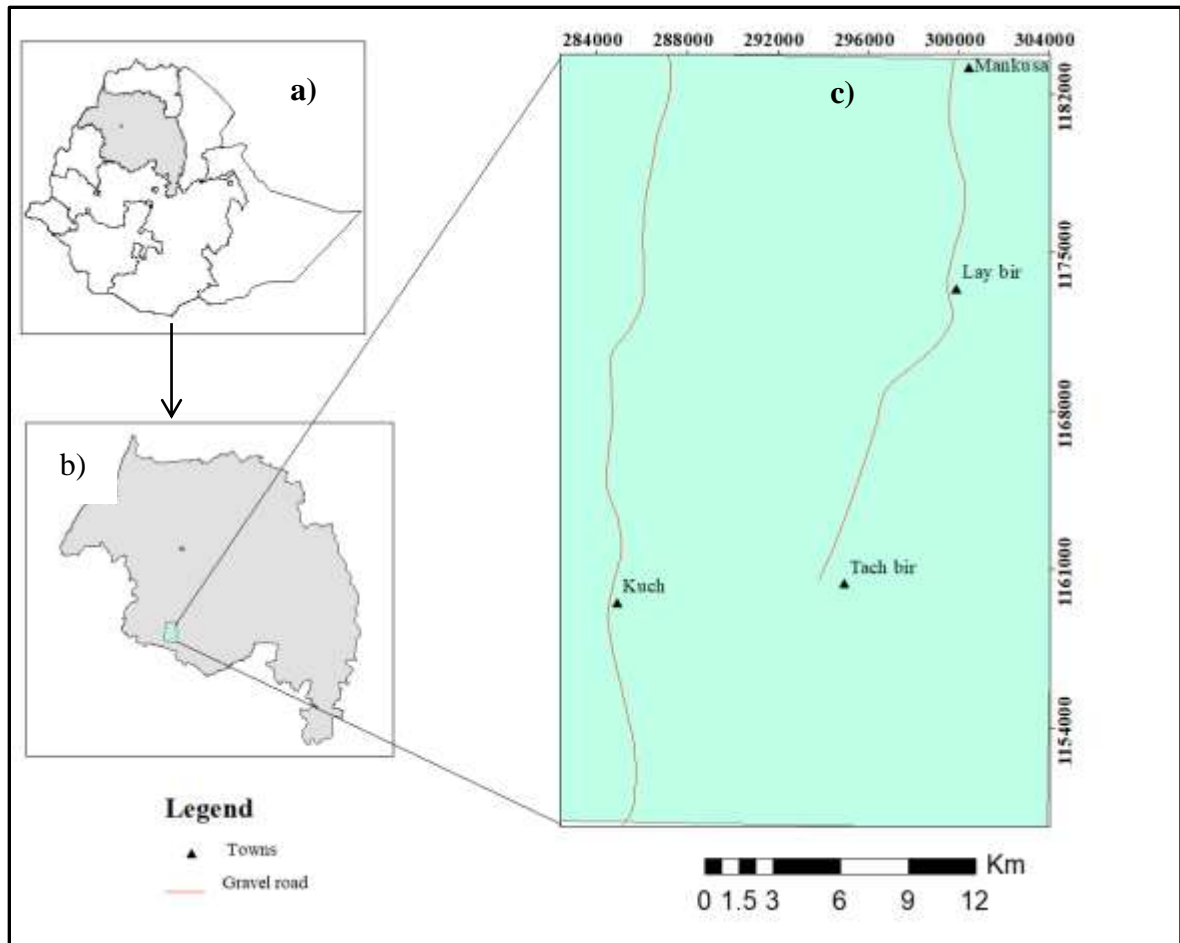


Figure 1.1) Location and accessibility map of the study area. a) Map of Ethiopia b) map of Amhara regional state c) Birsheleko area.

1.2.2 Physiography

In the study area, there is a V-shaped valley that is indicative of the presence of a deeply incised river (Birr River). That is responsible for the formation of alluvial deposits in the study area. The slope gradient also ranges from very gentle to very steep and most of the area has a very gentle to gentle slope. The horst of the valley is characterized by steep to the very steep slope and the graben of the valley is characterized by a very gentle slope. The maximum and minimum elevation in the study area is 2150 m and 1300m respectively. In general, most of the study area is characterized by rugged topography and low elevation morphologies (Fig. 1.2).

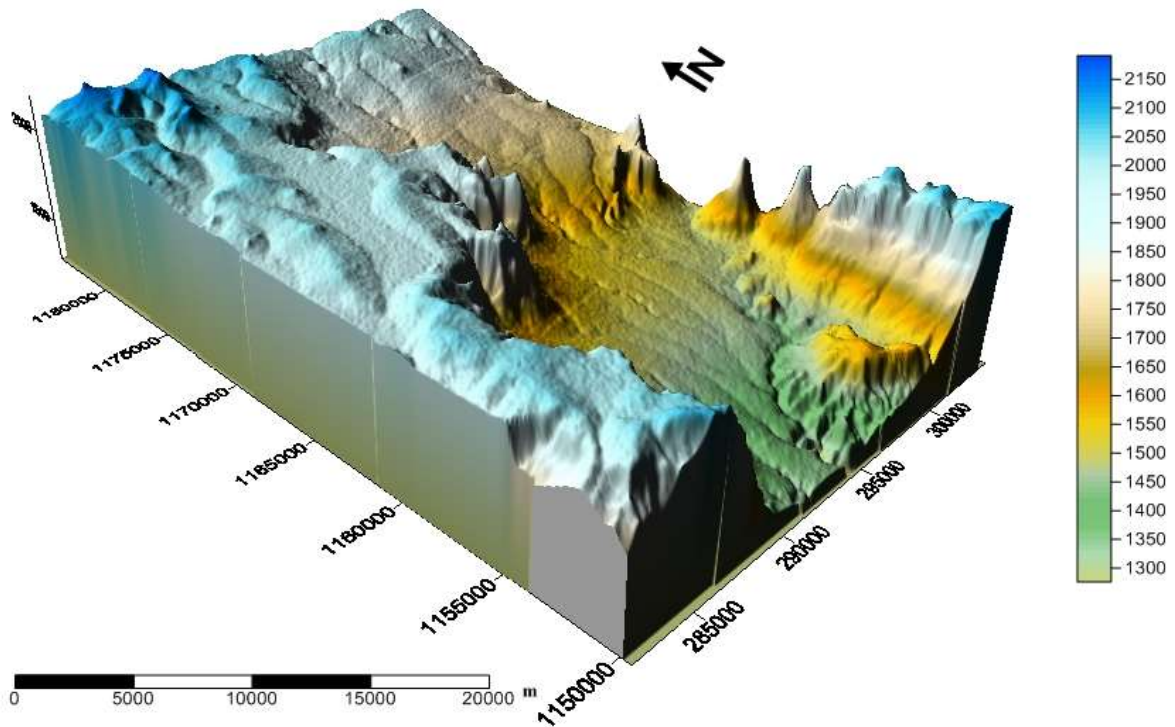


Figure 1.2) Physiographic map of the study area from DEM.

1.2.3 Climate condition

The climate of Ethiopia ranges from hot lowlands to cool highlands having an altitude that ranges from around 120 m below sea level in the Dallol depression, and up to 4620 m.a.s.l on the Semien Mountain highlands. Alemayehu, (2006) classified the Ethiopian climate into five climatic zones based on altitudinal range and temperature namely Bereha, Kola, Woina-Dega, Dega, and Kola. The Bereha zone is very hot having less than 500 m. a. s. l and above 25⁰C temperature, Kola zone is also a hot and arid region ranged between 500-1500 m.a.s.l. altitudes with 20-25⁰ C Woina-Dega, from 1500-2300 m.a.s.l and 15-20⁰C. Dega from 2300-3300 m.a.s.l with 10-15⁰C and Kur zones are found in highland regions having more than 3300 m.a.s.l and 10⁰C or less temperature. Accordingly, the study area is located between Woina Dega and Kola. It has a minimum and a maximum elevation of 1300 and 2150 m with an average elevation of 1725m. It is grouped under the Woyina Dega condition climate zone where the mean annual temperature is between 13⁰C and 29⁰C. In the study area the hottest month is March with a mean maximum temperature of 33⁰C and December is the coldest month having a mean minimum of 9.6⁰C. The corresponding maximum and minimum

average values are 29⁰C and 13⁰C respectively at Birsheleko (Lay Birr) station (Amhara Meteorological Agency, 1993-2016).

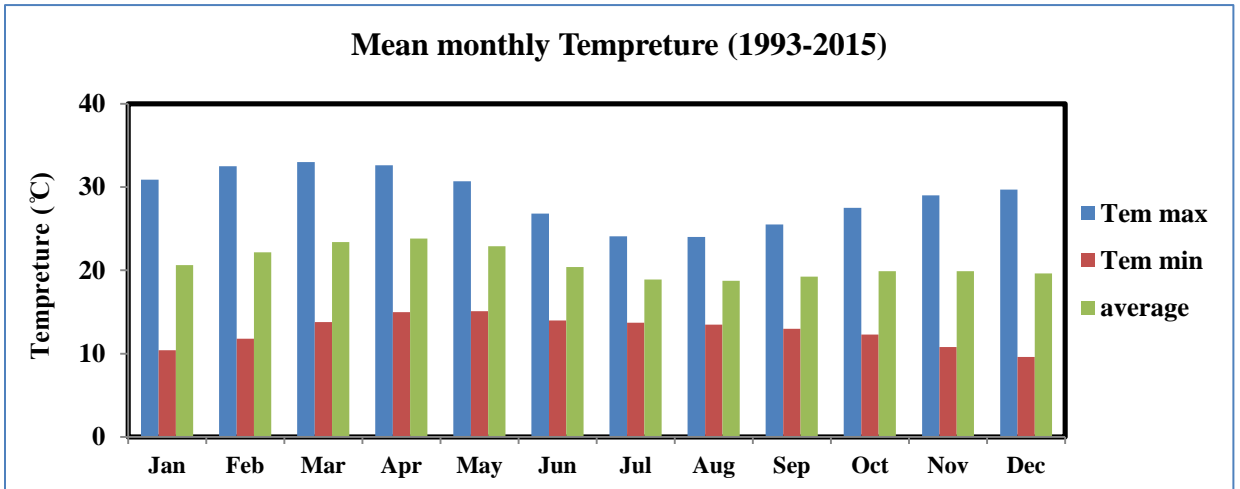


Figure 1.3) A bar chart that shows a mean monthly temperature of the Birsheleko area, data from (Amhara Meteorological Agency, 1993-2015).

The Birsheleko area has a unimodal pattern of rainfall. In general, the rainfall of the study area is characterized by its high variability in distributions. Meher or Kiremt is the rainy season that is largely received in the five months; May, June, July, August, and September. The average annual rainfall at Lay birr stations is about 1022.6 mm.

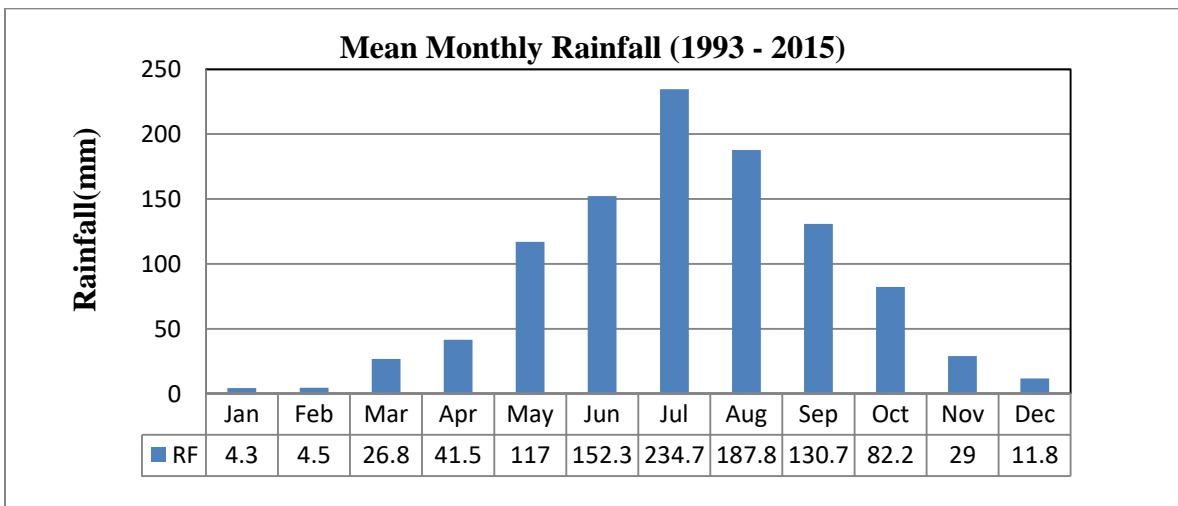


Figure 1.4) a bar chart that shows a mean monthly Rainfall of Birsheleko area data from (Amhara Meteorological Agency, 1993 -2015).

1.3 Objectives

1.3.1 General objective

The general objective of this study is to determine the Petrogenesis of volcanic rocks and associated mafic dykes in the Birsheleko area.

1.3.2 Specific objectives

The specific objectives of this research work are the following.

- ❖ To characterize and interpret the petrography and geochemistry of volcanic rocks and associated mafic dykes found in the study area.
- ❖ To evaluate the possible source and link of the volcanic rocks and associated mafic dykes of the area.
- ❖ To compare and contrast the result regionally with previous works in the Northwestern Ethiopian plateau and Main Ethiopian Rift (MER).

1.4 Statement of the problem and research questions

Most studies have been carried out at Ethiopian volcanism (e.g., Pik et al., 1998; Pik et al., 1999; Beccaluva et al., 2009; Ayalew et al., 2016; Hagos et al., 2016). Meshesha and Shinjo (2004, 2007) reported petrologic and geochemical data for Bure volcanic rocks (including the Birsheleko area) with a limited number of samples regionally. However, there were not enough representative samples taken from the Birsheleko area. Therefore, the new petrologic and geochemical data from Birsheleko volcanic rocks can potentially provide additional constraints regarding the characteristics of the Ethiopian Oligocene volcanics magma sources.

This research aims to study the petrology and geochemistry of Birsheleko area volcanic rocks and associated mafic dykes. These could also be used to investigate the geological processes involved in the genesis of the erupted magma and the characteristics of source composition which in turn, will be used to determine the Petrogenesis of the volcanic rocks of the target area. Moreover, it provides a geological map (at a scale of 1:50,000) and cross-section. Based on the objectives of the study the research questions to be examined and answered are:

- ✚ What are the lithological units of the study area? What kind of field relationship do they have,
- ✚ What are the sources of the volcanic rocks and the associated mafic dykes? Are they cogenetic or not?
- ✚ Is petrography, geochemistry, and source of volcanic rocks of the study area similar to volcanic rocks from previous works, which have been done in the Bure area, northwestern Ethiopian plateau, and main Ethiopia rift (MER)?

1.5 Methodology

To accomplish the objectives of this thesis work, the following methods were utilized. Field observation, petrographical studies, and geochemical data analysis have been done. All the collected data were organized, analyzed, and interpreted by using different software programs such as Microsoft Excel 2010, Surfer, GCDKit 4.1, Arc Map 10.1, and Global mapper 12.

1.5.1 Field investigation

Sampling and mapping were performed and the field traverses were primarily aimed for systematic sampling on rocks for petrographic and geochemical analysis. Rocks were collected and described at the outcrop-level, representative photographs of outcrop features were taken, and during traverses, an attempt was made to select representative samples.

1.5.2 Data analysis and organization

1.5.2.1 Petrographic analysis

A total of thirteen (13) thin sections were prepared in the mineralogy and petrography laboratory of the Geological Survey of Ethiopia (GSE). These thin sections were prepared by cutting the fresh part of the rock sample into an appropriate size by slitting each specimen with diamond saws. Then attached it to a glass slide and make it smooth and flat using progressively finer abrasive gravel until the exposed surface of the rock is gradually lapped down to 0.03 mm thickness. Regularly quartz is used as a standard measurement to determine the thickness since it is one of the most plenteous minerals, cemented it to microscope slides. A detailed petrographic study /thin section descriptions including mineral identification,

modal proportion estimation, textural descriptions, and rock naming were performed in the Bahir Dar University School of Earth sciences mineralogy and petrology laboratory.

1.5.2.2 Geochemical analysis

Based on spatial and lithological variation a total of 10 fresh samples were selected for whole-rock geochemical analysis. The sample preparation was accomplished at the ALS laboratory branch at Addis Ababa, Akaki Kaliti, Ethiopia, and send for geochemical analysis to Ireland. The samples were dried, crushed to 76.9% passing 2mm, slit, and pass through a splitter to got a 300-gram sample to which then fragmented to 93.3% passing 75 μm used for geochemical analysis. The concentration of major and selected trace elements in volcanic rocks was determined by a combination of methods (code: ME MS81d) Inductively Coupled Plasma-Mass Spectrometry (ICP-MS) and Inductively Coupled Plasma- Atomic Emission Spectroscopy (ICP-AES) both by disintegrating the sample by lithium metaborate (LiBO_2) fusion at the laboratory of Australian Laboratory Services (ALS), Ireland.

A 0.200 g prepared sample was added to 0.90 g lithium metaborate/ (LiBO_2) flux, blended well, and melt in an oven. The melt is then cooled and dissolved in 100 ml of 4% nitric acid (HNO_3), 2% Hydrochloric acids (HCl) solution. After extracting the ions from the plasma through a pinhole-sized cavity into a pumped vacuum system and focused with ion lens into a spectrometer. Finally, the solution is analyzed by Inductively Coupled Plasma-Mass Spectrometry for 30 trace elements. Besides, the same solution is then analyzed by ICP-AES and the results are emended for spectral inter-element interferences. The concentration of major oxides was calculated from the determined elemental concentration and finally the concentration of major oxides and trace elements i.e. the geochemical result was reported in the excel format (ALS, 2017). Major oxides (SiO_2 , Al_2O_3 , Fe_2O_3 , CaO , MgO , Na_2O , K_2O , TiO_2 , MnO , and P_2O_5) were analyzed with ICP-AES whole-rock package. Trace elements (Ba, Ce, Cr, Cs, Dy, Sm, Sn, Sr, Ta, Tb, Th, Tm, U, V, W, Y, Yb, Zr, Er, Eu, Ga, Gd, Hf, Ho, La, Lu, Nb, Nd, Pr, Rb) were analyzed with a whole-rock package of Lithium Borate Fusion by ICP-MS. Besides, base metals (Ag, As, Cd, Co, Cu, Li, Mo, Ni, Pb, Sc, Ti, and Zn) were analyzed by with ICP-AES acid digestion. The reproducibility of the analyzed results was checked by using blank and duplicated samples. Accuracy of major oxides is $<3\%$; those of trace elements are $<5\%$.

1.6 Expected outcome and significance of the research

As mentioned in the statement of the problem the Birsheleko area has not been studied in the aspect of petrology and geochemistry locally. The main expected research outputs will be the following:

- ❖ Geological map of the study area at a scale of 1:50,000 and geologic cross-section.
- ❖ A detailed description of the petrography of the studied rocks.
- ❖ An interpretation of the Petrogenesis of the volcanic rocks and associated mafic dykes based on the geochemical and petrographic analysis.

The study will have a benefit to geologists who want geological data of Birsheleko area volcanic rocks and associated mafic dykes including, petrographic and geochemical data either to conduct further studies or for their purpose.

CHAPTER TWO

2. REGIONAL GEOLOGIC SETTING

2.1 The Ethiopian continental flood basalt

The Ethiopian continental flood basalt comprises the triple junction of Afar, where the Red Sea, the East African Rift System, and the Gulf of Aden connect (Mohr and Zanettin, 1988). It is one of the youngest flood basalts in the world with estimated areal coverage of about 750,000 km² before the erosion and 600,000 km² after the occurrence of the erosion (Mohr, 1963 as cited by Mohr and Zanettin, 1988). Having a thickness that varies from 700 to 2000m and a total volume of about 350,000 km³ (Mohr, 1983; Ayalew and Yirgu, 2003; Kieffer et al., 2004). It is exposed overlying unconformably on the Mesozoic sedimentary units or the Pan-African crystalline basement (Beccaluva et al., 2009).

The earliest Eocene volcanism in Ethiopia is mainly restricted in the southern and southwestern parts of Ethiopia, having an age of about ~45 Ma (George et al., 1998) also within the Northwestern Ethiopian plateau. The eruption of the flood basalts occurred in less than five million years with the highest eruption rates occurring from 28 to 31 Ma (Hofmann et al., 1997; Pik et al., 1998; Meshesha and Shinjo, 2007). Then this continental flood volcanism has been widespread throughout Ethiopia and Yemen regions linked with subordinate felsic pyroclastic rocks (Hofmann et al., 1997; Pik et al., 1998, 1999; Ayalew et al., 2002; Ayalew and Yirgu, 2003; Kieffer et al., 2004; Ayalew et al., 2016). Volcanism in Ethiopia has been commonly explained as bimodal (Mohr, 1983). Based on their lithological development, age of effusion, volcanic activity, and frequency of volcanic centers the volcanic rocks have been classified into five major provinces (Abbate and Sagri, 1980). These are volcanics of the northern plateau, southern plateau, Somalian plateau; Afar volcanics, and Main Ethiopian Rift (MER) volcanics. The first three groups comprise the major part of the Ethiopian volcanites and named the trap series (Merla et al., 1979 and Abate and Sagri, 1980). The rest two groups are collectively called the Aden series (Abate and Sagri, 1980).

2.2 Volcanics of Northwestern Ethiopian plateau

The Ethiopian volcanic plateau is separated into the Northwestern plateau and Southeastern plateau by the Ethiopian rift valley (Asrat et al., 2012). The Northwestern Ethiopian plateau is described by Oligocene Pre rift volcanic rocks overlying by Miocene volcanoes (Mohr and Zanettin, 1988; Pik et al., 1998). It is composed of several specific volcanic centers with different magmatic characters and with a large range of ages (Kieffer et al., 2004). The major volcanic units of the Western Ethiopian Plateau (WEP) are the Oligocene flood volcanic (Trap series) i.e. (Oligocene–Miocene basalts and rhyolites), Miocene shield volcanoes, Volcanic plugs, and Quaternary volcanic rocks (Dercq et al., 2001; Peccerillo et al., 2003; Kieffer et al., 2004).

The eruption of enormous flood lava sequences (Peccerillo, 2007) is characterized by basaltic lava flows, basaltic tuffs, as well a considerable volume of rhyolitic, trachytic, and phonolitic products (Mohr and Zanettin, 1988). The first stage of volcanism is known as the Aiba and Ashangae formation, recognized as the bimodal basalt- rhyolite type (Chazot and Bertrand, 1993), a feature common to most continental flood basalt provinces (e.g., Parana and Karoo). A homogenous mineralogical composition is observed in the Ethiopian flood basalt mostly they have aphyric to sparsely phyric texture containing phenocrysts of plagioclase, clinopyroxene \pm olivine. Like the mineralogy, they also have uniform chemical composition mainly ranges from tholeiitic to transitional chemical composition (Mohr, 1983 and Pik, et al., 1998).

Pik et al (1998) classified the flood basalts of the Northwestern Ethiopian region into three, types; the Low Titanium (LT), High Titanium-1 (HT1), and high Titanium -2 (HT2) based on their HFSE concentration. The high Titanium basalts are found in the southeastern sector of the plateau and low Titanium basalt exposed in the Northwestern sector. Despite the predominance of basalts, the flood volcanics (Trap series) contains significant volumes of felsic volcanic rocks mostly friable tuffs, rhyolites, and ignimbrites. They are found interlayered with the flood basalt especially in the upper part of the sequence (Mohr and Zanettin, 1988; Pik, et al., 1998; Ayalew and Yirgu, 2003).

The formation of large shield volcanoes (e.g., Mt. Semien and Gugufu) is the second stage of activity after the occurrence of the flood basalt, also known as Termaber formation (Mohr, 1971; Kieffer et al., 2004; Peccerillo, 2007). Similar to the flood basalts the shield volcanoes are bimodal; however, they are more porphyritic having many and frequently large Olivine and plagioclase phenocrysts, tholeiitic and alkaline composition. Besides they are thinner and less continuous than the underlying flood basalts (Kieffer et al., 2004).

In the Northwestern Ethiopian plateau alkali rich, silica saturated trachytic volcanic plugs are found that are believed to be associated with the overlying shield volcanoes but, are not feeders of the flood basalt (Dercq et al., 2001). The third stage is Quaternary in age, related to the Tana rift that is a volcanic activity including Lake Tana (Mohr, 1971). Volcanic cones, Scoriaceous basalts, Basanites, Tephrites, Phonolite, Nephelites, and Alkali basalts were found (Mohr 1971; Merla, 1979; Abate et al., 1998). These volcanic units having a Quaternary alkaline chemical affinity of basaltic lava flows with some trachytes and they are grouped in a Pleistocene age. Furthermore, Hofmann et al. (1997) noted that the host lavas are basanites in composition and its age around 0.39 ± 0.03 Ma.

The study area is found in the western part of the northwestern Ethiopian plateau, which has been considered as part of the Bure area by using the geochemical and petrographical study by Meshesha and Shinjo (2004; 2007). It is also a part of the geological map of the Bure map sheet (NB-37/5) at the scale of 1:250,000 compiled by Tsige and Haile, (2007). Based on petrochemical composition, the mode of occurrence compositions, and stratigraphic composition volcanic rocks of the Bure are classified into stratified basalts (lower and upper basalts), recent basalts, scoria cones, agglomerate, trachyte flows, and trachyte plugs (Meshesha and Shinjo, 2004). Geochemically the Bure area volcanic rocks are composed of transitional tholeiitic and alkaline continental flood basalts (Meshesha and Shinjo 2004; 2007).

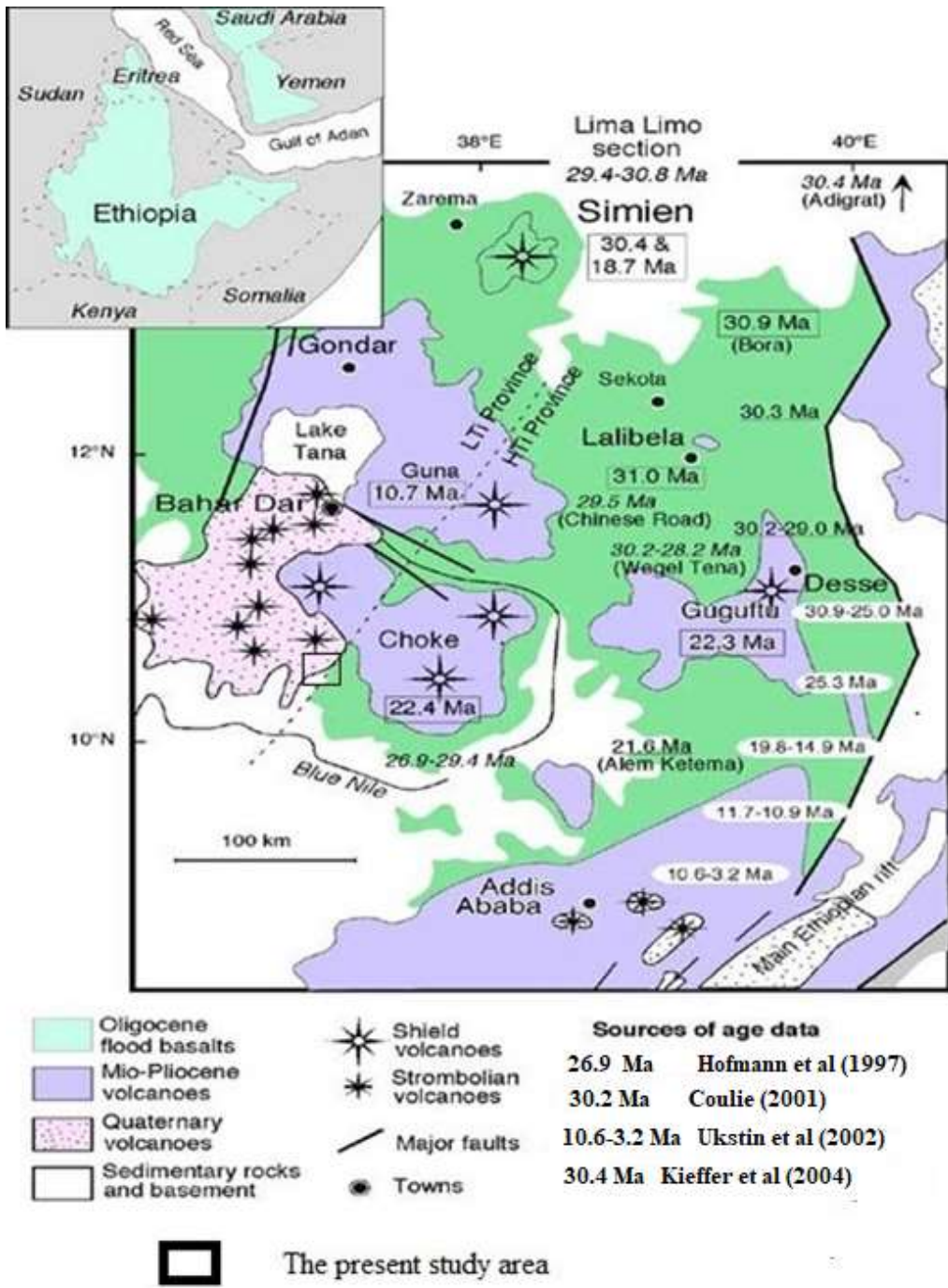


Figure 2.1) Geological map of the central and Northwestern Ethiopian plateau showing the extent of the flood volcanism (Adopted from Kieffer et al., 2004).

CHAPTER THREE

3. GEOLOGY OF THE STUDY AREA

3.1 Lithological description

The study area is covered by Cenozoic volcanic rocks unconformably overlying on the Neo-Proterozoic basement (granitoids) rocks and Mesozoic sedimentary rocks. The rocks are classified based on petrography, field description, chemical composition, and mode of occurrence into basalt, dolerite, basaltic andesite, and scoria cones.

3.1.1 Basalt

Most of the study area is covered by the basaltic lava flow, exposed in the area by forming gently to moderately steep topographic features and rarely short cliffs. Texturally, basaltic rocks in the study area can be classified as aphanitic, vesicular, amygdaloidal, and porphyritic. In most parts of the studied area, fresh basalts have been observed; however, in some parts of the area highly weathered and commonly jointed features are identified.

The aphanitic basalts in the study area are exposed by a quarry site, hillside, and river cut. The weathered part of the rock is characterized by grey to dark, and red to yellowish color due to oxidation of its mafic minerals to hematite and other iron oxides, while the fresh part of the rock has a grey to dark color. Besides, a fine-grained vesicular basalt having black to grey fresh and weathered color, showing sub-rounded, elliptical, and elongated shape vesicles are also observed. Furthermore, amygdaloidal basalt is filled by secondary minerals such as calcite and quartz found in the study area exposed by river and road cut. Among the lithological units found in the study area the porphyritic basalt, vesicular basalt, and the amygdaloidal basalt cover a very small portion so that they are not mappable with the scale of the map.

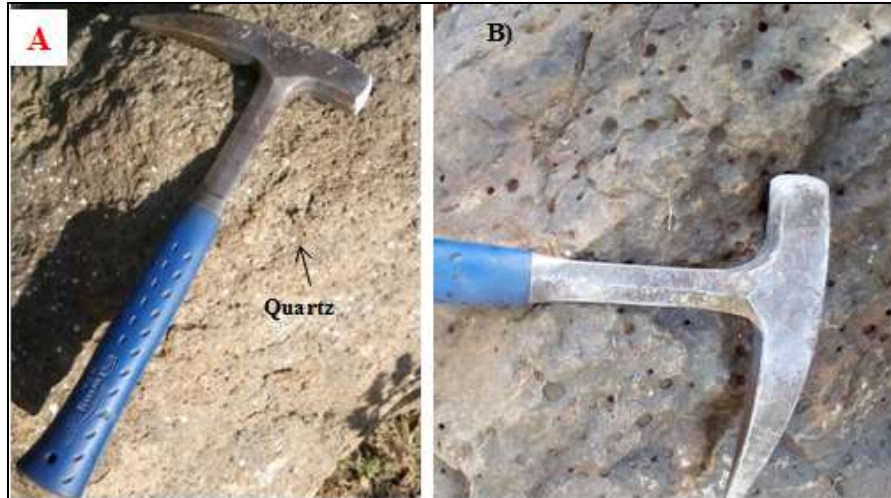


Figure 3.1 a) Amygdaloidal basaltic rock units with vesicles filled by quartz exposed by a river b) Vesicular basalt.

3.1.2 Basaltic Andesite

This rock unit is exposed as a dyke around ‘Gedame Iyesus’ church cutting through the basaltic rocks (Fig 3.1). It is characterized by layered features and shows a flow banding structure. The fresh part has a black and grey color, while the weathered part has a light brown color. The strike of the flow is N10 W; the dip is towards the southeast.



Figure 3.2) Field photograph of (sample code BS-5) basaltic andesite which is exposed as dyke around Gedame Iyesus church.

3.1.3 Dolerite

This rock unit is situated below Horoseka elementary school following the gravel road from Kuch to Birsheleko (Fig 3.1). It shows a dark grey color and also contains medium grain size crystals. This shallow intrusive crystalline igneous rock shows typical spheroidal weathering

(exfoliation), which is the shivel of rocks into a series of concentric shells by subsequent weathering processes. It is exposed as dyke cutting through highly weathered basaltic rocks.

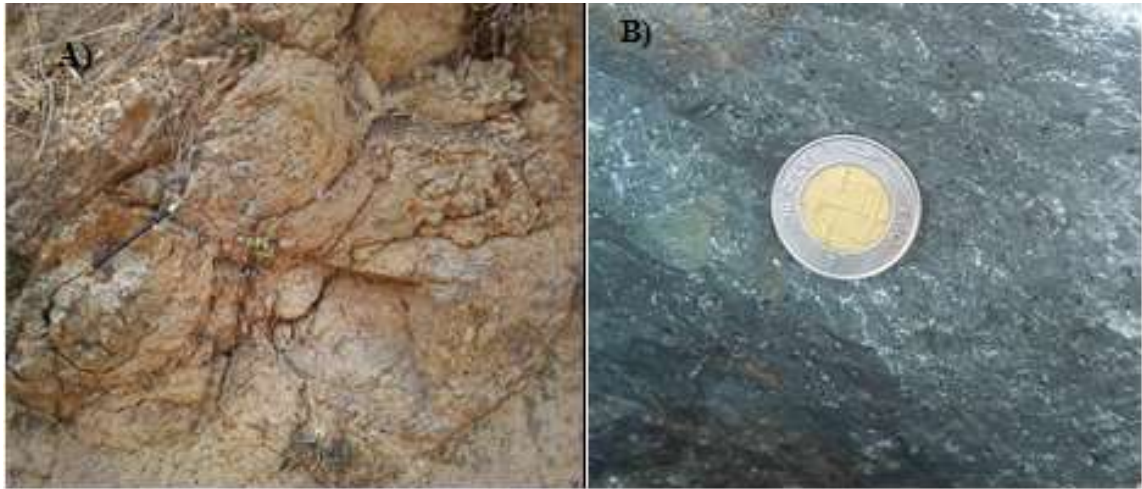


Figure 3.3) a) Field photograph of a dolerite rock unit showing exfoliation b) dolerite (sample code BS-11).

3.1.4 Scoria cones

The scoria cones are found as rock fragments overlying on the basaltic flow. Because the cones quarried for road and other construction purposes created a half breached morphology and have moderate to steep slopes. The pyroclasts show various colors in outcrops such as light gray, dark gray, greenish-gray, light brown, yellowish-brown, reddish-brown, pink, and purple varieties. Ash, lapilli, and block /bomb size loosely compacted grains found with a variety of shapes. A thin layer of scoriaceous basalt having black and a grey fresh color, reddish and brown weathered color is found in the study area. It shows a small degree of weathering relative to the underlying basalts and is exposed by filling the lower topography of the valley .

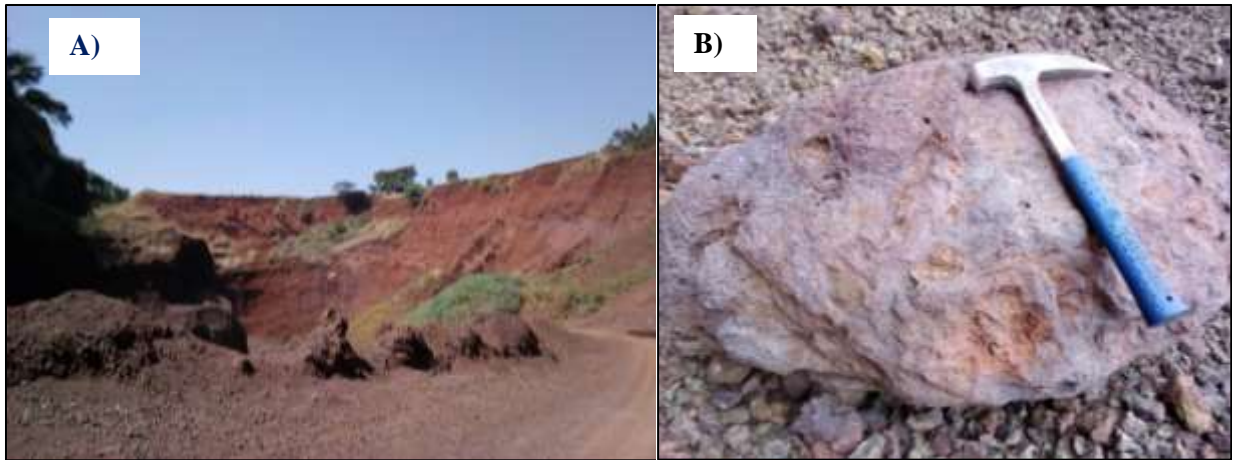


Figure 3.4 A) Field photograph of scoria cone showing a half breached morphology. B) Volcanic bomb.

3.2 Petrography

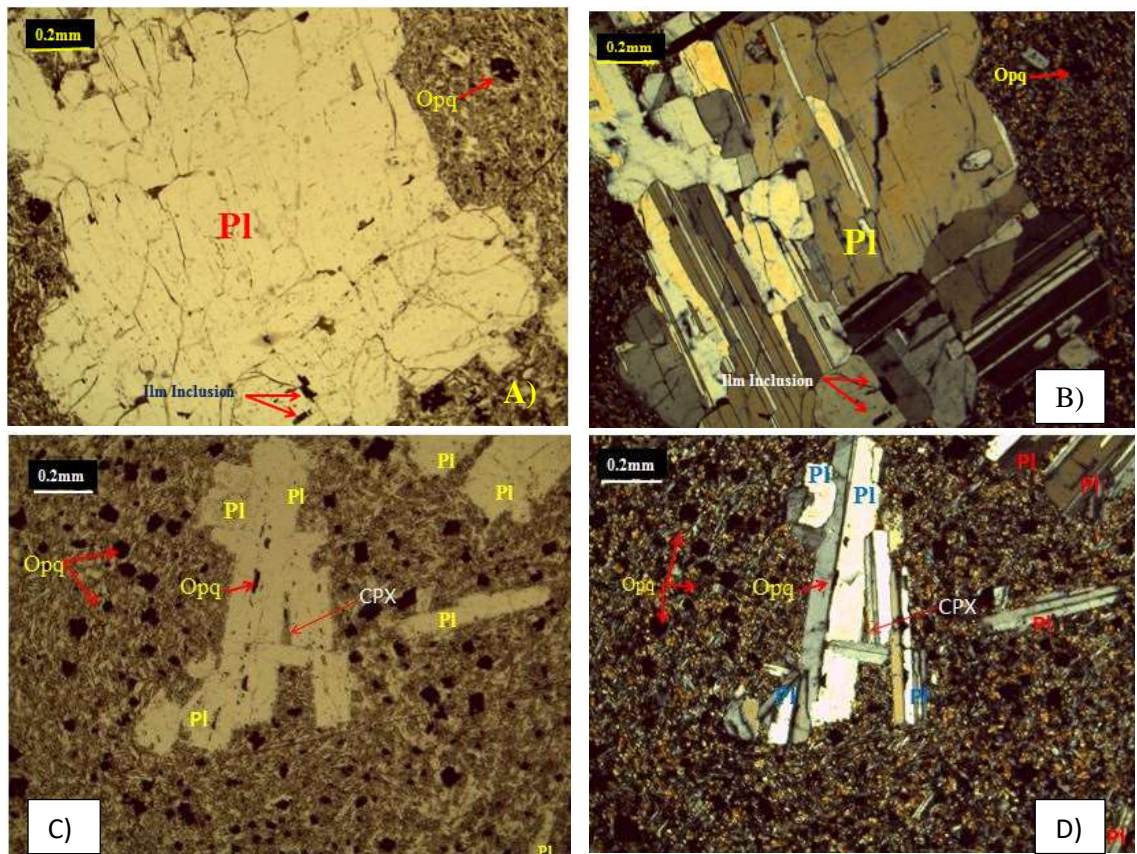
The aim of studying petrography is to describe and systematically classify rocks. Based on petrographic studies modal mineralogical compositions of rocks i.e. the percentage of essential minerals and sequence of mineral formations can be detected (Winter, 2014). These data are commonly used to give petrological conclusions about the type of textures and mineral assemblages, and its cooling history of the magma. One of the most common methods in petrography is a modal analysis which helps to determine the essential constitute minerals in the rock. Accordingly, 13 (thirteen) thin sections were investigated under the plane Polarized (PPL) and crossed polarized (XPL) view by using a transmitted light microscope. Based on their texture observed under a microscope (micro-texture) the studied samples are classified into porphyritic and aphyric. Again based on modal mineralogical abundance the porphyritic rocks are classified into Olivine phyric basalt, Pyroxene phyric basalts, and Plagioclase phyric basalts and dolerites. The aphyric samples are further classified into aphyric trachy flow basalt and aphyric trachy flow basaltic andesite.

3.2.1 Plagioclase phyric basalt and dolerite

This rock unit is characterized by the porphyritic texture when plagioclase covers the greatest percentage. Rocks with sample code **BS-1**, **BS-7**, **BS-10**, are basalts that have Plagioclase phyric texture. Sample codes **BS-11** and **BS-2** are samples taken from dolerite dyke having Plag phyric texture. The groundmass is composed of plagioclase laths, Opx and Cpx, and Fe-Ti oxide minerals, and have microphenocryst of orthopyroxene crystals. The interstitial

texture is observed in sample code **BS-7** (Fig3.5: C and D).The interstice of plagioclase phenocryst which shows like A shape is filled by clinopyroxene (Augite). Sometimes plagioclase phenocrysts occur as mega phenocryst with a length greater than 3mm having orthopyroxene as inclusion (in sample code **BS-1** see (Fig 3.7 G)).

Sample code **BS-1** and **BS-10** are composed of 30% phenocrysts (28% lath Euhedral plagioclase, and 2% clinopyroxene), 70 % groundmass lath-shaped Plagioclase, pyroxene (augite), and opaque minerals). Sample code **BS-7** (Fig. 3.7.D) has 20% plagioclase (phenocryst), and 80% (groundmass consists augite, plagioclase and opaque mineral (magnetite and ilmenite)). Sample **BS-11** has a 25% plagioclase phenocryst and 75% groundmass. The groundmass is composed of the same mineral as the rock samples expressed above.



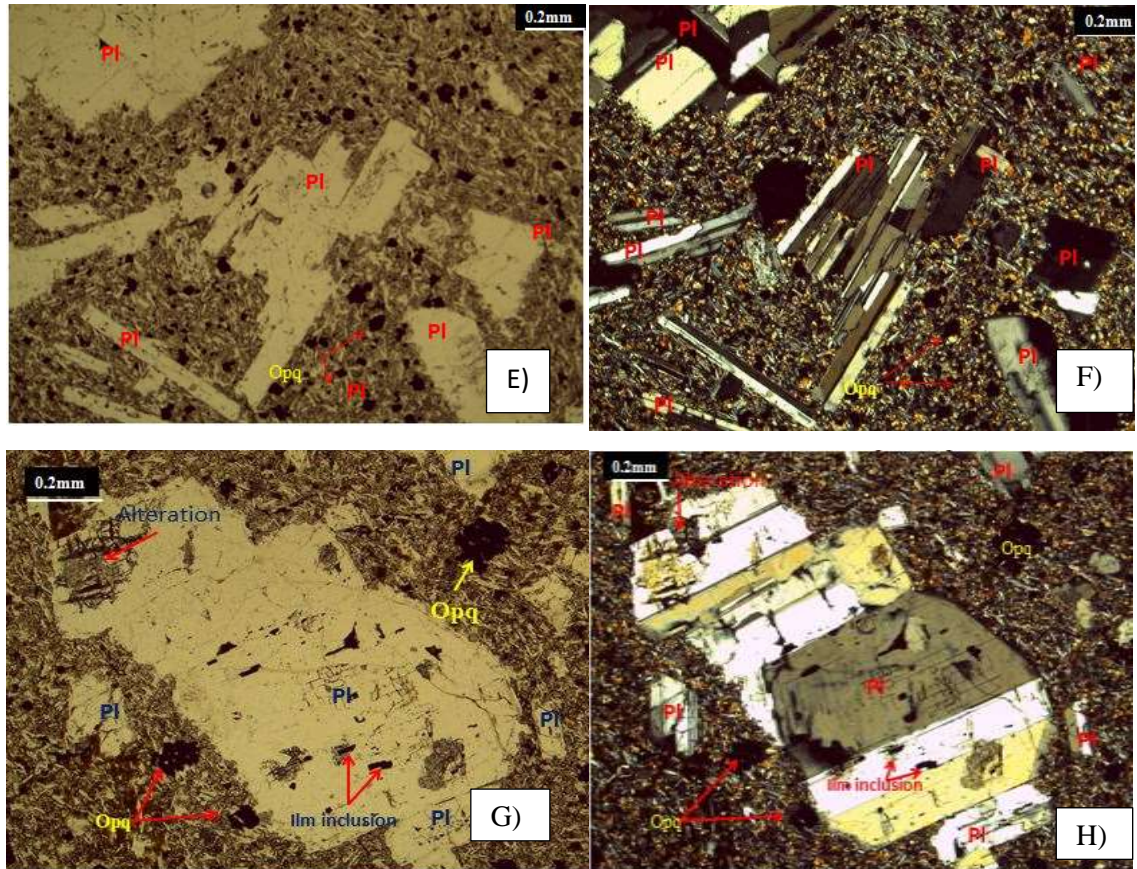


Figure 3.5) Thin section photomicrographs of the plagioclase phyric basalt and dolerite rock units. Sample BS-11 having a 2mm sized plagioclase phenocryst with Ilmenite inclusion set in groundmass under PPL (A) and XPL (B). Sample BS-7 under PPL (C and E) and XPL view (D and F); sample BS-1 under PPL (G) and XPL view (H). Note; Pl is Plagioclase feldspar, Ilm is Ilmenite, Opq is opaque minerals. All the images are taken under 4x magnification power. Abbreviations of minerals name are after Whitney (2010).

3.2.2 Pyroxene phyric basalt

Even though pyroxene and olivine present as phenocryst pyroxene (clinopyroxene) have the greatest volume percentage during the modal analysis due to this reason the rock is named pyroxene phyric basalt. Olivine and clinopyroxene occur as phenocryst while the groundmass is consists of pyroxenes, olivine, plagioclase, and opaque minerals. Zoned clinopyroxenes also present as phenocryst. Commonly, half sector zoning (due to the presence of the triangle) and oscillatory zoning are the dominant features shown in this rock unit (Fig. 3.8). Sample code **BS-13** is pyroxene phyric basalt. Sometimes inclusions of Cpx are also found within the Cpx phenocryst. Petrographically, this lava flow comprises the glomeroporphyritic aggregates of ferromagnesian minerals.

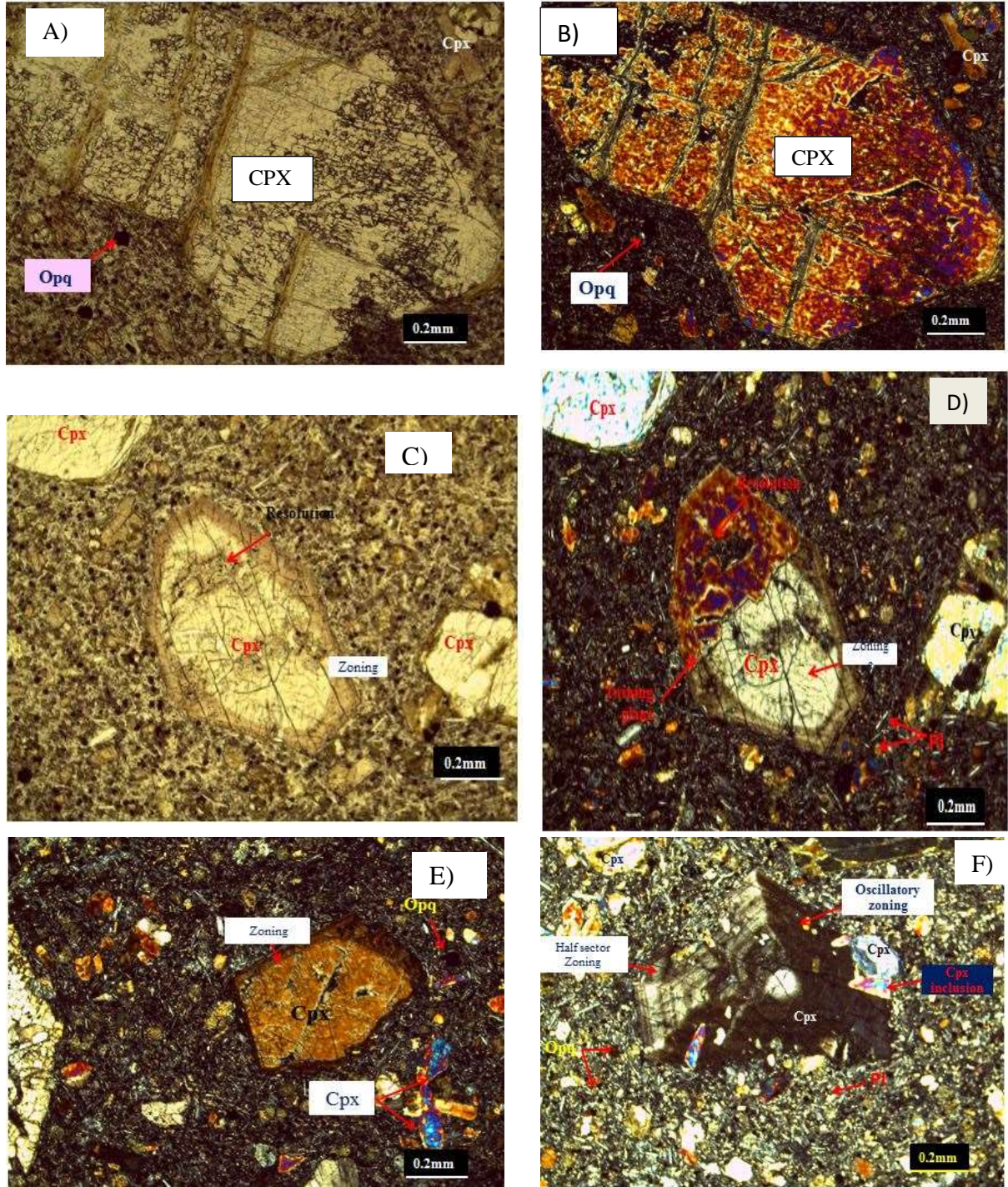
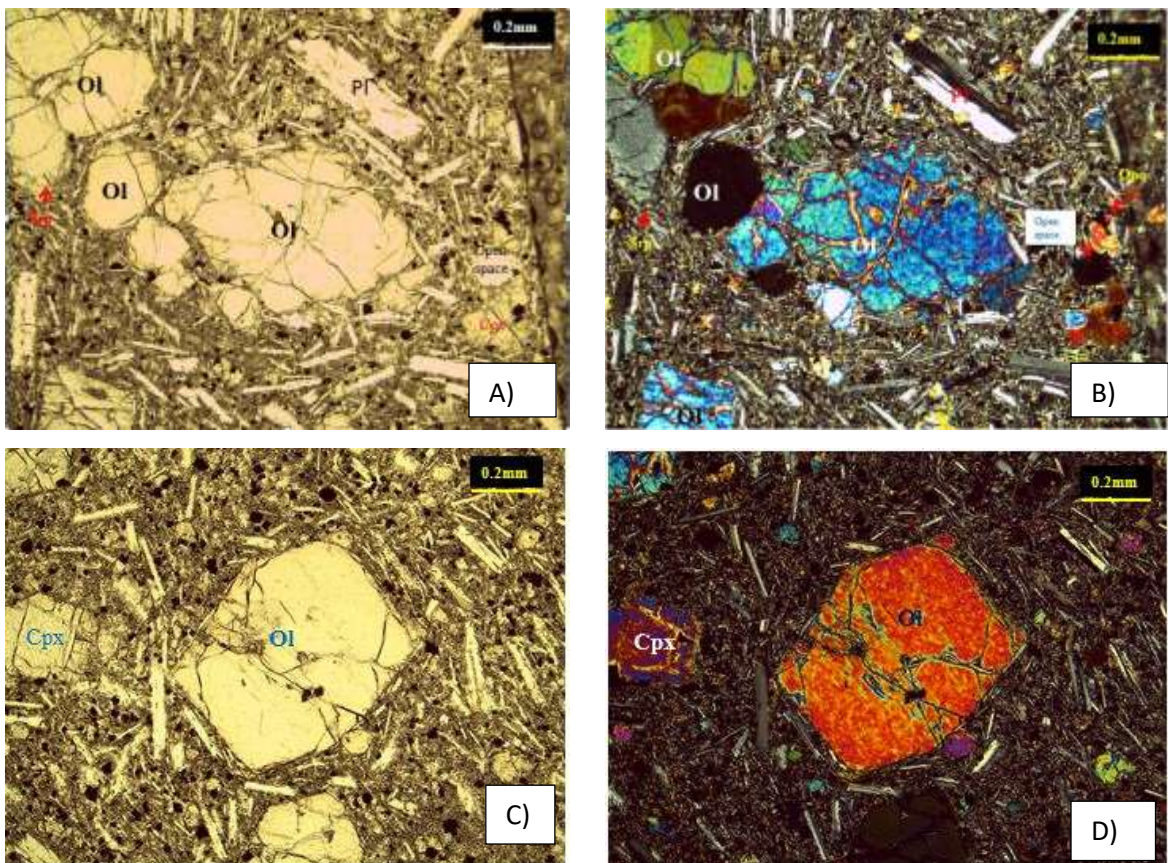


Figure 3.6) Thin section photomicrographs of the pyroxene phyric basalt rock unit (BS-13). *Opq* phenocryst with a resorption feature under PPL (A) and XPL (B). *Cpx* phenocryst having resolution features showing zoning and twinning under PPL(C)and XPL(D). *Cpx* phenocryst with zoning and *Cpx* microphenocryst rest in groundmass under XPL (E) view. *Cpx* phenocryst with oscillatory and half sector zoning (F). All the images are taken under 4x magnification power. Note; *Pl* is a plagioclase

feldspar, *Opq* is opaque minerals. *Cpx*: clinopyroxene, *Opx*: orthopyroxene Abbreviations of minerals name are after Whitney (2010).

3.2.3 Olivine phyric basalts

Sample code **BS-9**, **BS-6**, and **BS-12** are olivine phyric basalts composed of olivine and pyroxene phenocrysts. Clinopyroxene, plagioclase, and opaque (iron titanium oxides) present as groundmass. Olivine is surrounded by spinel crystals and clinopyroxenes glomeroporphyritic and resorption textures are also observed. In sample code, **BS-9** olivine crystals show strong alteration and became anhedral in shape. The skeletal texture is observed in some plagioclase crystals.



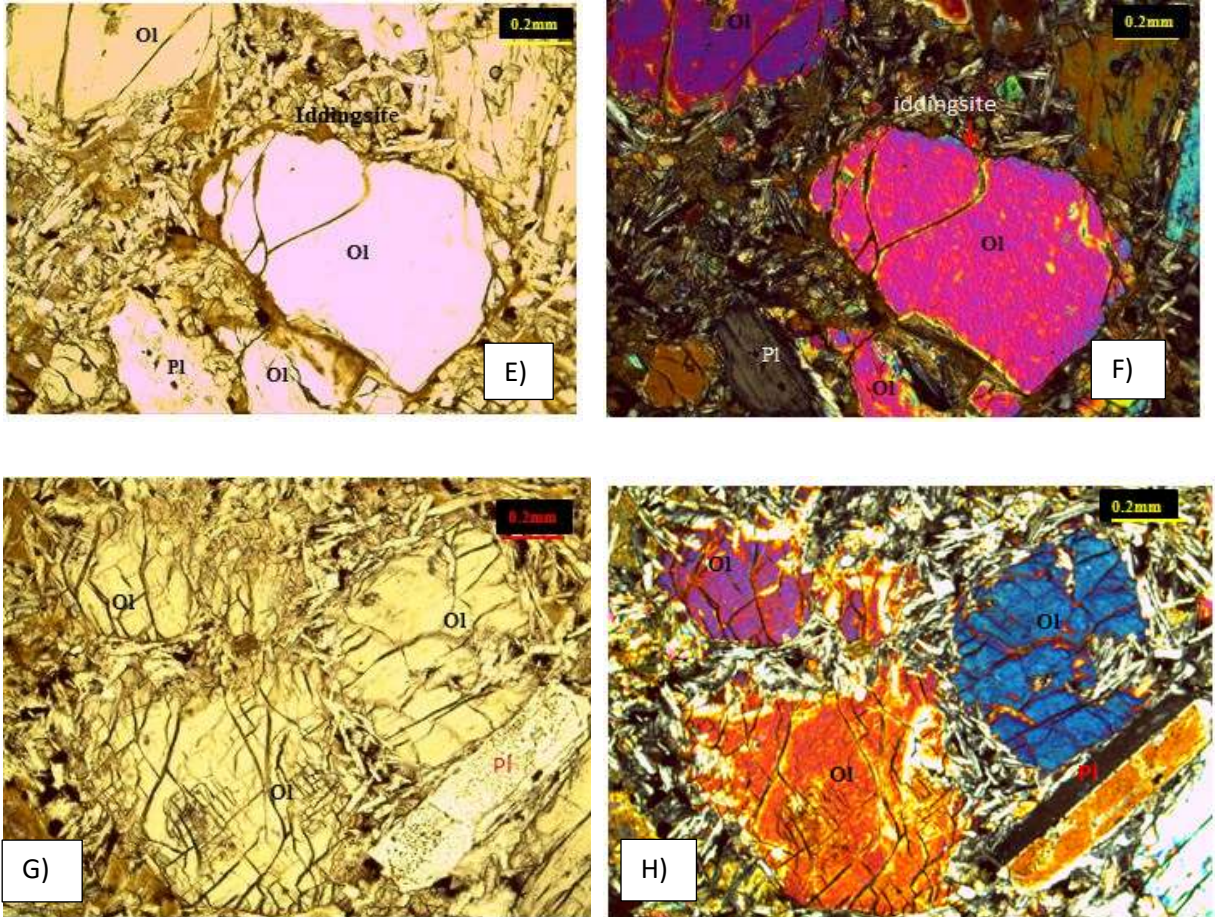


Figure 3.7) Thin section photomicrographs of the Olivine phyric basalts. Euhedral Ol phenocryst, Pl phenocryst, Cpx microphenocryst having Cpx inclusion set in the groundmass, alteration of olivine into Serpentine i.e chrysolite (sample BS-9) under PPL(A) and XPL(B). Subhedral Ol phenocryst with inclusion surrounded by Cpx, Pl microphenocryst set in groundmass (sample Bs-9) under PPL(C), and XPL (D). Subhedral olivine phenocryst altered to iddingsite along the rim i.e showing corona texture, Pl phenocryst with Opq inclusion (sample BS-12) under PPL (E), and XPL (F). Phenocryst of Ol and Pl (sample Bs-12) set in groundmass under PPL (G) and XPL (H). All the images are taken under 4x magnification power. Note; Pl is a plagioclase feldspar, Ol; olivine; Opq is opaque minerals, Cpx: clinopyroxene, Opx: orthopyroxene, Sp: serpentine. Abbreviations of minerals name are after Whitney (2010).

3.2.4 Aphyric-trachy flow basalt and basaltic andesite

Plagioclase micro phenocrysts are found in association with distinguishable minerals in the groundmass level with dominant plagioclase crystals. In the groundmass: plagioclase, Fe-Ti oxides, and minute Cpx minerals are observed. Further, plagioclase micro phenocrysts are elongated and euhedral. The arrangement of plagioclase micro phenocrysts is rarely

radiating, but they have sub-parallel to parallel orientations. Sometimes, it slightly shows intergranular groundmass textures. However, the overall texture observed in this rock is trachytic and the rock name is established based on the dominant plagioclase microphenocryst alignments. Sample code **BS-4** and **BS-5** are aphyric–trachy flow basaltic andesites. Sample code **BS-3** and **BS-8** are basalt samples that show aphyric trachy flow texture under thin section observation (see Fig.3.10a), containing a few lath-shaped plagioclase micro phenocrysts (1-2 vol %) set in a groundmass that consists of similar minerals with the aphyric trachy flow basaltic andesites.

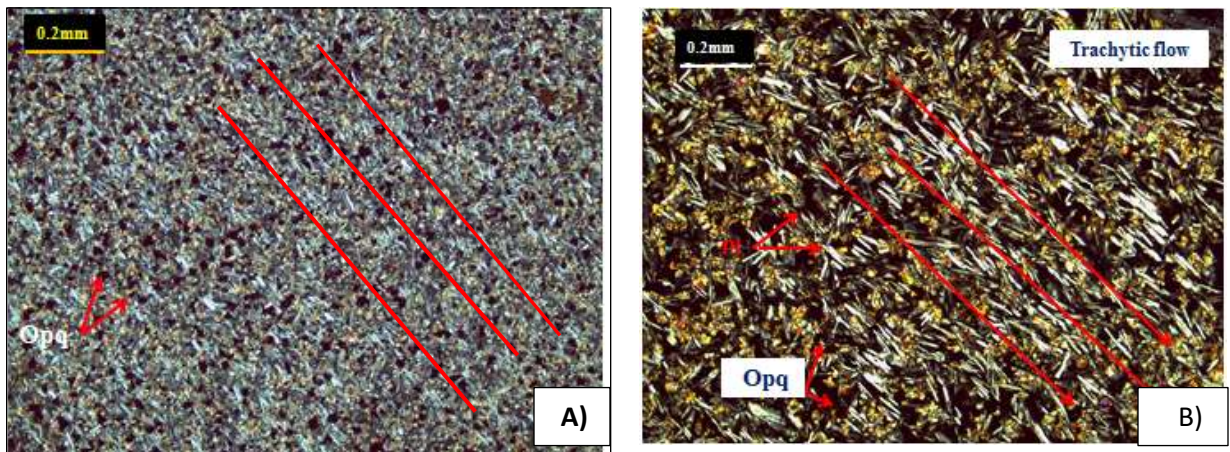


Figure 3.8) Microphotographs of a) Aphyric trachy flow basalt under XPL (sample BS-3), b) aphyric trachytic basaltic andesite showing trachytic flow (XPL) (sample BS-4). The images are taken under 4x magnification power. Note; opq is opaque minerals Abbreviations of minerals name are after Whity (2010).

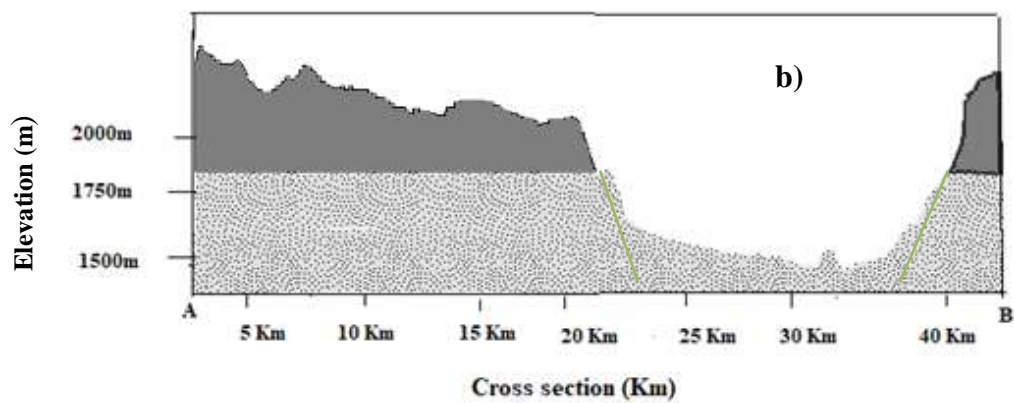
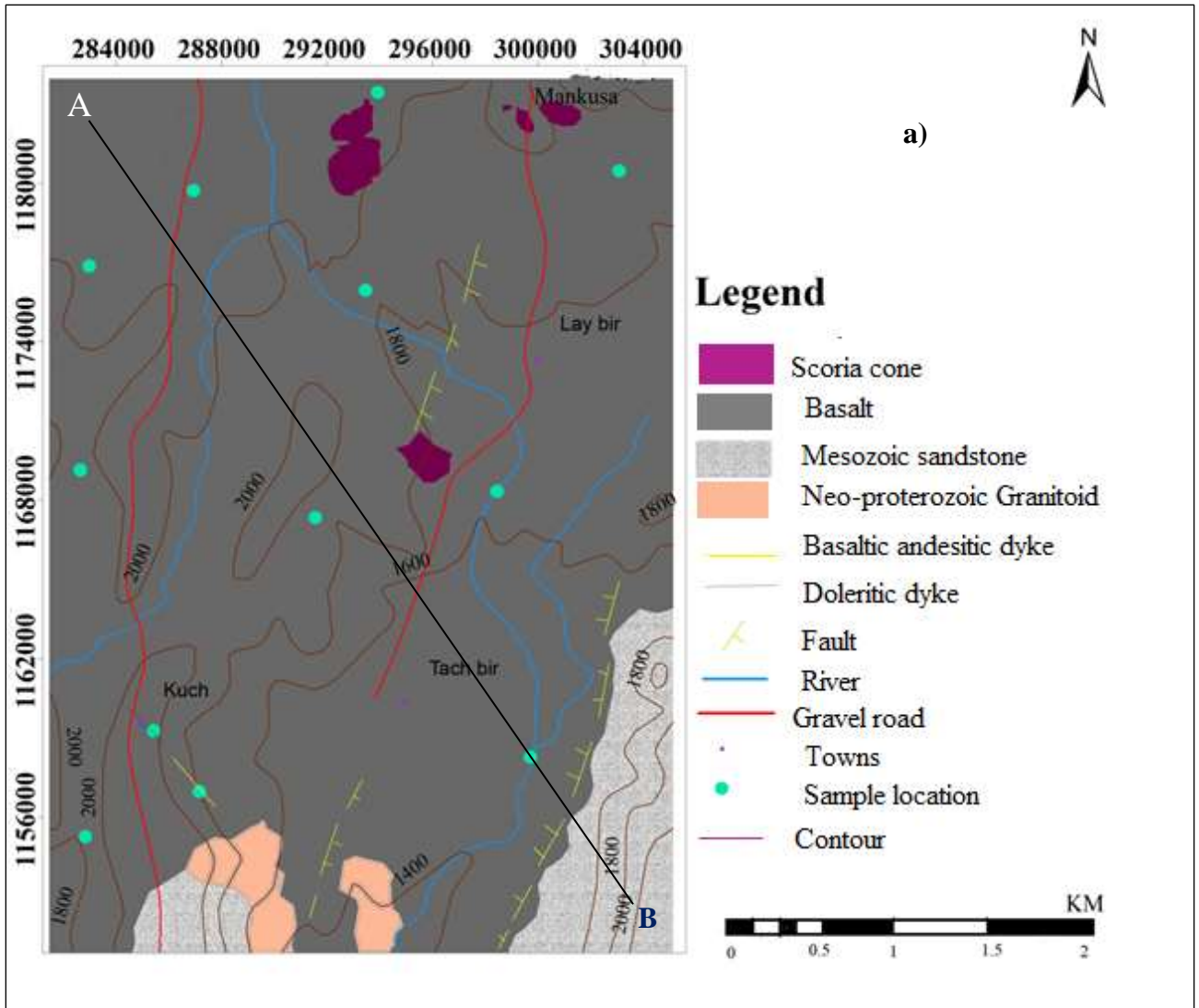


Figure 3.9 a) Geological map of the study area at a scale of 1:50,000. b) Cross-sectional profile (A-B) of the study area with a normal fault.

3.3 Geological structures

Geological structures can be primary or secondary structures. Primary structures are structures that formed during the rock formation process and secondary structures are structures formed after the rock formed (Spry, 1962 as cited in Phillips et al., 2013). The layering (flow banding), observed in the basaltic andesite, and the columnar joint shown in the basalt are primary structures found in the study area. Besides, joints, faults, and dykes which are classified under secondary structures also found in the study area. The dykes and flow banding are discussed with the lithological unit description section while in this section the joint and fault are described.

3.3.1 Joint

Joints are the dominant geologic structures found in the study area and it affects most of the basaltic rock units, having diverse morphology. In general, there are two dominant trends of the joints NW-SE and NE-SW which characterize most of the joint populations. In the study area columnar, orthogonal, and X joints are observed.

3.3.2 Fault

The valley landform helps us to recognize the presence of faults. Normal faults with NE-SW orientation are common. The NE-SW inferred geological faults are traced from ASTER DEM.

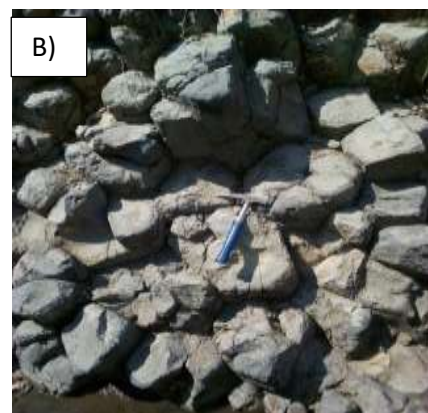




Figure 3.10) a joint on a basalt. A) Having a strike of N60W, dip amount of 50. B) Afield photograph showing columnar basalt exposed by Inbodbod river. C) X joint having a dip amount of 47 and a strike of S 22 E.

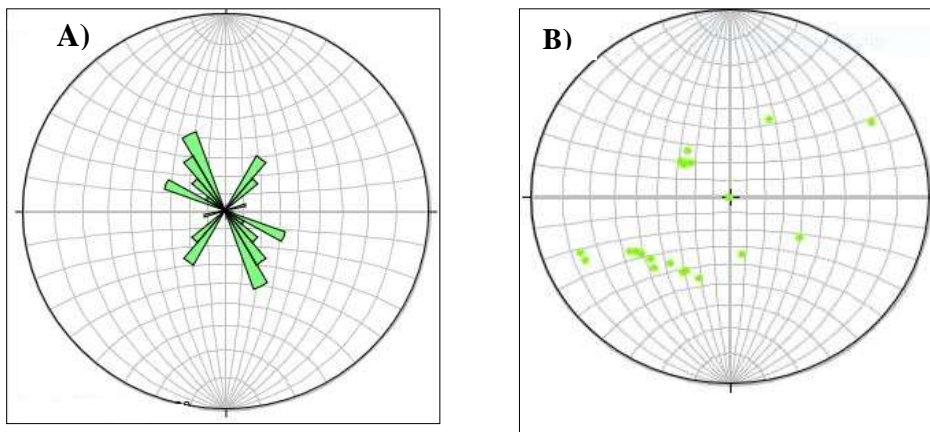


Figure 3.11) (A) Rose diagram Strike of the joints. (B) Equal angel plot of joints in the form of a pole that was taken from different exposures.

CHAPTER FOUR

4. WHOLE ROCK GEOCHEMISTRY

4.1 Introduction

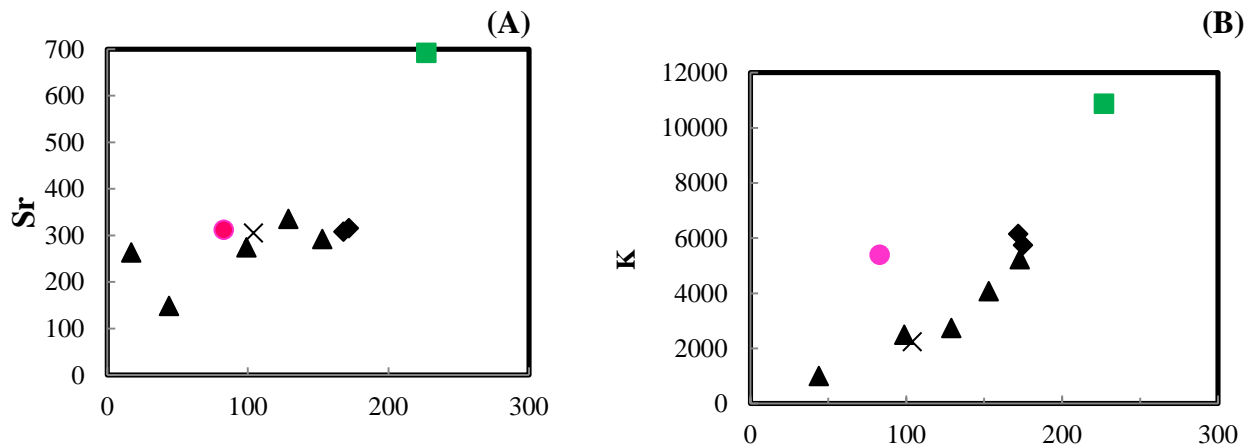
Whole-rock geochemistry is the best method used to study the magmatic evolution of any volcanic product including fractional crystallization, the degree of partial melting, and different magmatic processes (Huss et al., 2010). It mostly depends on the relative signature of the elemental composition that helps to understand the geologic process. Because major elements are mainly used to divide igneous rocks and study the chemical evolution of melts during the crystallization. The concentration of trace elements is important to determine magma sources (Winter, 2014).

According to Rollinson (1993), there are four major categories of geochemical Data namely radiogenic isotope, stable isotope, major elements, and trace elements. Of the four categories, only two of them (major and trace) are used in this study. Major and trace element geochemical data types are used to understand the evolution of magma. Besides, the volatile content (e.g., H₂O), which is a type of major element geochemical data and presented as Loss of Ignition (LOI) is used only to know the behavior and alteration effect on mobile elements. LOI represents the total volatile content of the rock that is determined by igniting the rock with a temperature of 105 °C.

The geochemical results are reported in Tables 4.1, 4.2, and 4.3. If the total of the analyzed sample varies between 98.8 wt % and 100.8 wt %, it is considered to be acceptable (Best, 2003). The total of analyzed samples ranges from 98.83 to 100.42 wt. % and the loss on ignition (LOI) range from 0.1 to 2.02 wt. %, it is considered as acceptable content. Several variation diagrams for major element oxides versus MgO and trace elements Vs MgO were constructed (Figs. 4.1, 4.2, and 4.3) respectively. Chondrite normalized rare earth elements (REE) abundance patterns (Fig. 4.4) and primitive mantle normalized incompatible trace elements patterns or spider diagrams (Fig. 4.5) are also plotted for the volcanic rocks of the study area. Normalization values are from Sun and McDonough (1989).

After crystallization, igneous rocks may be affected by compositional alteration as a result of interaction with groundwater, seawater, or hydrothermal fluids (Cox, 1979). The LOI value ranges from 0.1 to 2.02 which is supported by the petrographic observation that most of the samples are less altered. However, alteration of olivines and pyroxenes was observed. To know whether they are affected by alteration or not their chemical variation has to be examined before using the geochemical data for interpretation using the alteration index. Alteration Index ($AI = 100(MgO + K_2O) / (MgO + Na_2O + CaO + K_2O)$) about 35 ± 10 are generally accepted to be characteristics of volcanic rocks (Laflièche et al., 1992). Based on this suggestion basaltic rocks in the study area have low AI values, ranging from 28-44%.

The LILE (K, Rb, Ba, and Sr) are mobile elements, so their abundance can be modified during alteration and low-grade metamorphism (Winter, 2014). An immobile trace element such as Zr and Th are used to check the mobility of other trace elements because they are immobile and appears not to be modified during alteration and low-grade metamorphism (Pearce, 1982). As shown in the diagram (Fig. 4.1) K, Ba and Rb show a positive correlation with Th and Zr. These trends suggest that the relative immobility of those elements during post-solidification processes. Sr is scattered in both Zr and Th (Fig. 4.1: A and E) indicating its mobility. Generally, this trend indicates to use for interpretation.



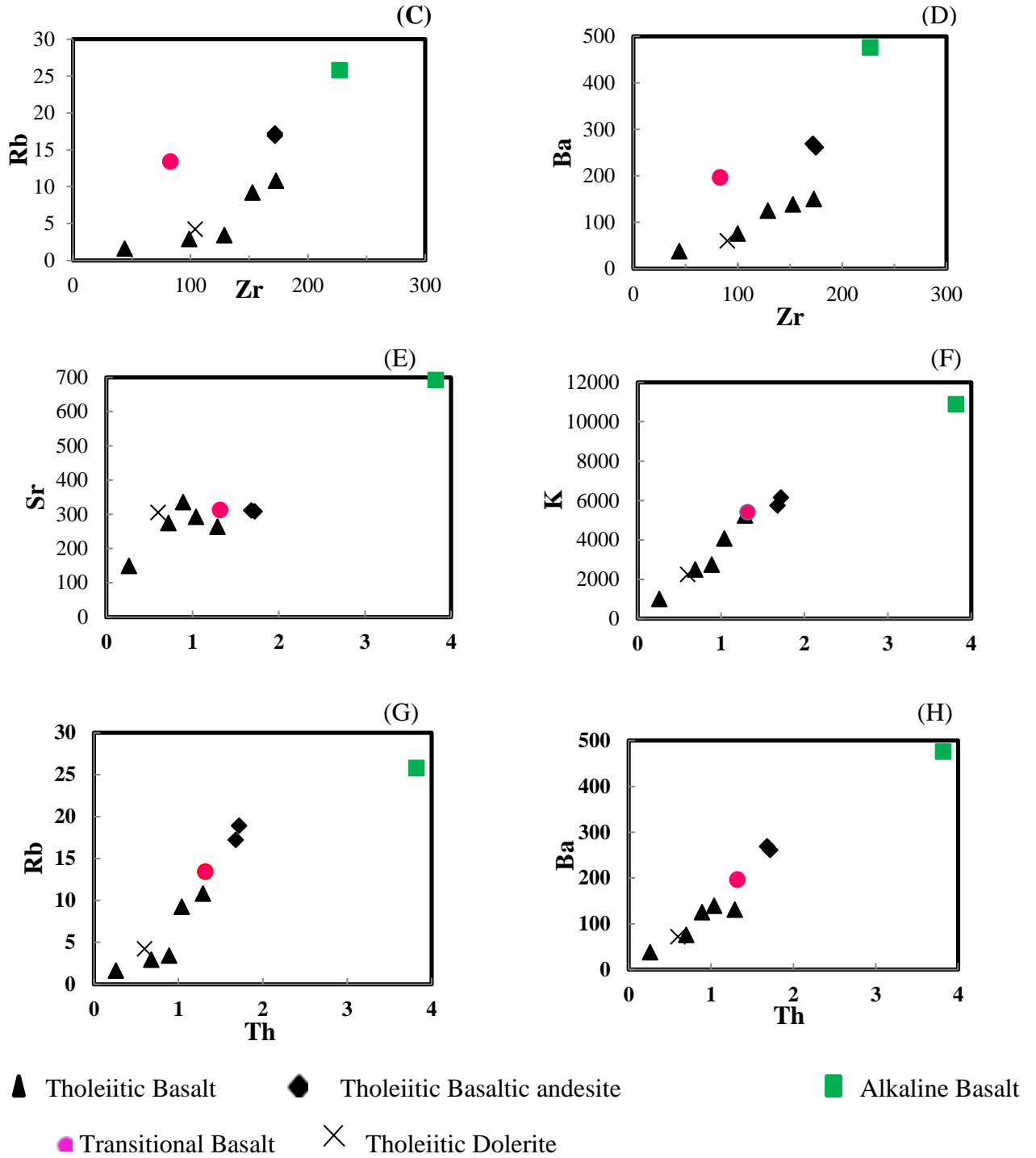


Figure 4.1) selected trace elements vs. Zr and Th diagrams for checking element mobility during post-eruptive alteration after Zhang et al. (2008).

Table 4.1) Major oxide concentration in (wt. %) for representative samples from the Birsheleko area volcanic rocks and associated mafic dykes.

S. code	BS-1	BS-4	BS-5	BS-7	BS-8	BS-9	BS-10	BS-11	BS-12	BS-13
Rock Type	Basalt	Basaltic Andesite	Basaltic Andesite	Basalt	Basalt	Basalt	Basalt	Dolerite	Basalt	Basalt
SiO₂	49.0	52.1	51.9	50.3	49.9	47	49.2	49.5	45.3	44.9
TiO₂	1.53	2.03	2.01	1.96	2.35	1.17	1.93	1.45	0.79	2.01
Al₂O₃	17.05	13.75	13.7	15.15	13.55	14.2	15.9	17.69	11.9	14.45
Fe₂O₃	10.55	14.1	14.05	12.3	14.25	12.35	12.25	10.2	9.12	10.5
Mno	0.15	0.2	0.2	0.19	0.19	0.17	0.17	0.15	0.13	0.17
MgO	5.42	4.29	4.39	5.66	5.16	11.7	5.45	5.55	16.35	9.56
K₂O	0.3	0.75	0.79	0.49	0.63	0.65	0.33	0.27	0.12	1.31
CaO	12.0	8.6	8.51	10.85	9.04	9.45	11.2	12.53	11.5	10.5
Na₂O	2.3	3.14	3.09	2.56	2.78	2.89	2.52	2.12	0.96	3.23
P₂O₅	0.13	0.22	0.23	0.18	0.25	0.24	0.19	0.12	0.06	0.52
LOI	0.87	1.18	0.95	0.1	0.72	0.1	0.84	0.15	2.02	1.64
Total	99.44	100.42	99.88	99.58	98.83	99.9	100.07	99.69	98.86	99.48
FeO_t	9.4	12.6	12.4	11.0	12.7	11.9	10.9	9.1	8.1	9.3

Table 4.2) Trace elements concentration in (ppm) for representative samples from the Birsheleko area volcanic rocks and associated mafic dykes.

S. code	BS-1	BS-4	BS-5	BS-7	BS-8	TBS-9	BS-10	BS-11	BS-12	BS-13
Rock Type	Basalt	Basaltic Andesite	Basaltic Andesite	basalt	Basalt	Basalt	Basalt	Dolerite	Basalt	Basalt
La	6.1	13.5	13.00	8.90	10.9	12.9	9.0	6.0	2.6	36.1
Ce	15.4	32.1	31.6	22.7	27.4	25.7	23.3	15.9	7.2	68.6
Pr	2.12	4.66	4.54	3.2	3.85	2.98	3.06	2.21	1.03	7.57
Nd	11.20	21.6	21	15.4	18.7	12.2	15.8	11.6	5.3	29.8
Sm	3.03	5.81	5.66	4.31	5.21	2.58	4.04	3.42	1.58	5.85
Eu	1.22	1.93	1.98	1.58	1.92	1.07	1.39	1.2	0.57	1.94
Gd	3.77	6.89	6.61	5.27	5.96	3.33	4.81	3.61	2.03	4.95
Tb	0.60	1.10	0.95	0.81	0.99	0.49	0.7	0.57	0.33	0.73
Dy	3.87	6.91	6.73	5.37	6.25	3.13	4.59	3.83	1.91	4.28
Ho	0.73	1.30	1.30	1.00	1.17	0.63	0.91	0.73	0.40	0.82
Er	2.18	3.56	3.71	2.87	3.57	1.80	2.50	2.04	1.14	2.39
Tm	0.32	0.50	0.52	0.38	0.49	0.26	0.38	0.33	0.19	0.33
Yb	1.75	3.44	3.11	2.32	3.03	1.65	2.06	1.8	0.96	1.96
Lu	0.25	0.54	0.51	0.34	0.41	0.25	0.33	0.26	0.14	0.32
V	247	337	333	325	375	162	319	263	171	187
Cr	70	30	30	50	20	520	100	70	1460	410

Ni	56	19	21	45	27	316	57	60	569	176
Cs	0.04	0.15	0.2	0.12	0.13	0.12	0.01	0.03	<0.01	0.32
Rb	2.9	17.2	18.8	9.2	10.8	13.4	3.4	4.2	1.6	25.8
Ba	75.4	269	261	139	130.5	196.5	125	71.7	37.4	476
Sr	274	308	311	292	263	312	335	305	148.5	692
Th	0.68	1.72	1.68	1.04	1.29	1.32	0.89	0.6	0.26	3.82
U	0.26	0.47	0.44	0.43	0.54	0.29	0.31	0.24	0.09	0.96
Nb	4.1	7.5	7.2	7.1	8.3	21.0	7.2	4.6	2.03	50
Ta	0.2	0.3	0.25	0.32	0.4	0.7	0.2	0.1	<0.1	2.9
Zr	99	172	177	153	173	83	129	110	44	227
Hf	2.7	4.6	4.4	3.9	4.4	1.7	3.3	2.5	1.3	4.7
Eu/Eu*	1.1	0.93	0.99	1.02	1.05	1.12	0.96	1.04	0.97	1.1

* Total Fe as FeO (Desta et al., 2015).

FeO= Fe₂O₃ * 0.89 (Rollinson, 1993).

Eu/Eu*= Eu_N/√Sm_N*xGd_N (Rollinson, 1993), subscript N denotes normalized to Chondrite (Sun and McDonough, 1989).

Table 4.3) CIPW norm calculations in (wt. %) for the Birsheleko area volcanic rocks and associated mafic dykes.

Rock Name	Basalt	Basaltic Andesite	Basaltic Andesite	Basalt	Basalt	Basalt	Basalt	Dolerite	Basalt	Basalt
S. code	BS-1	BS-4	BS-5	BS-7	BS-8	TBS-9	BS-10	BS-11	BS-12	BS-13
Q	6.2	11.09	10.48	7.59	9.38	0	6.61	5.3	0	0
Or	1.78	4.43	5.61	2.89	3.72	3.84	1.95	1.59	0.7	7.74
Ab	19.5	26.57	26.14	21.66	23.5	24.45	21.32	19.2	8.12	23.97
An	35.3	21.2	20.7	28.39	22.63	23.85	31.09	37.85	27.8	21.06
Ne	0	0	0	0	0	0	0	0	0	1.81
Di	14.5	10.69	10.73	14.14	10.33	14.539	13.36	14.85	20.71	15.42
Hy	6.78	5.73	5.95	7.54	8.06	6.33	7.38	6.73	19.9	0
Ol	0	0	0	0	0	11.26	0	0	7.86	11.67
Il	0.32	0.42	0.42	0.4	0.4	0.36	0.36	0.32	0.27	0.36
Hm	10.55	14.1	14.05	12.3	14.25	12.35	12.25	10.2	9.12	10.5
Tn	3.34	4.43	4.38	4.28	5.24	2.4	4.26	3.14	1.58	0
Pf	0	0	0	0	0	0	0	0	0	3.09
Ap	0.3	0.52	0.54	0.42	0.54	0.521	0.45	0.33	0.14	1.23
Sum	98.54	99.2	99	99.6	98.1	99.9	99.	99.5	96.2	96.8

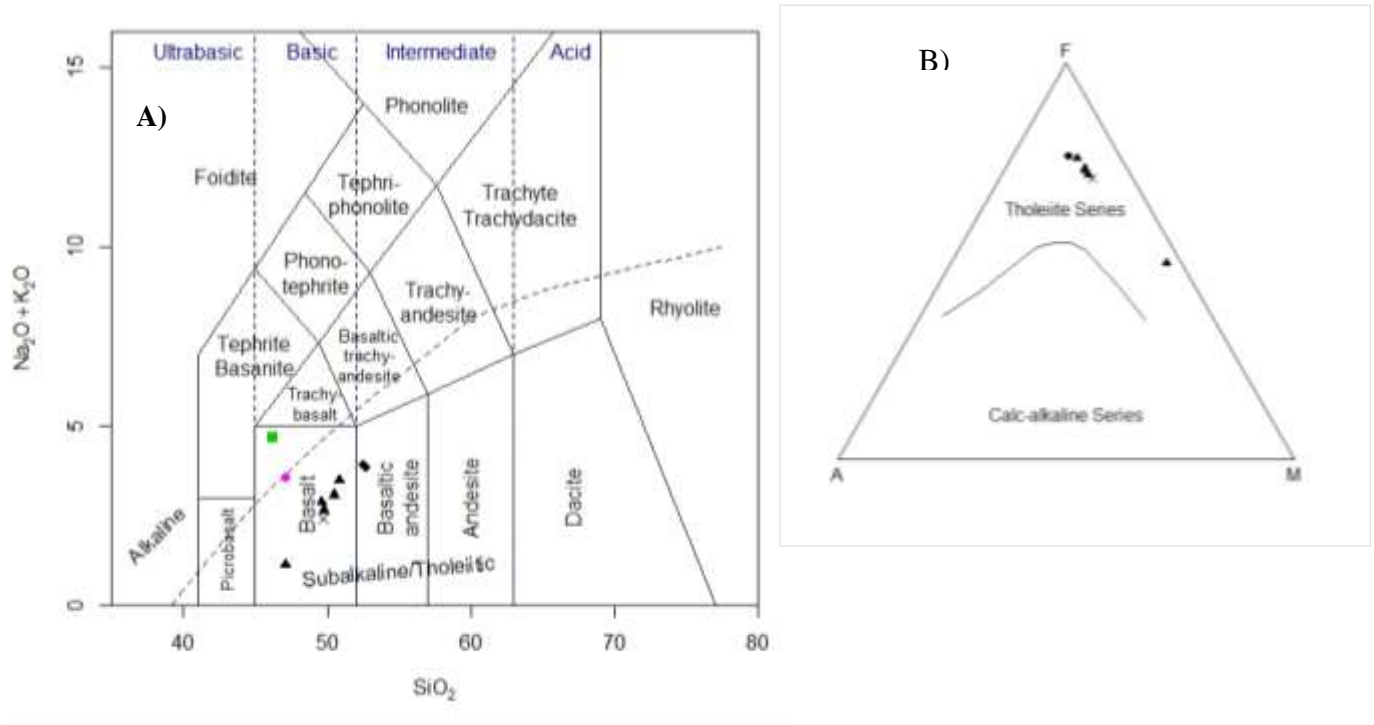
For normative calculation $Fe_2O_3/FeO = 0.15$ is used.

Note that; **Q**: quartz; **Or**: orthoclase; **Ab**: albite; **An**: anorthite; **Ne**: nepheline; **Di**: diopside; **Hy**: hypersthene; **Ol**: olivine; **Il**: Ilmenite; **Hm**: hematite; **Tn**: tenorite; **Pf**: Perovskite; **Ap**: apatite.

4.2 Major elements geochemistry and rock classification

The source and process of rock formation will be analyzed by examining the concentration of major elements at the preliminary level (Winter, 2014). The distribution from the TAS classification diagram shows that the occurrence of mafic and intermediate rocks. Out of ten samples, two samples fall on the basaltic andesite group. while the rest samples are fall on the basalt (Fig. 4.2 A). From the studied samples, one rock sample falls in the alkaline magma series; besides, one sample grouped in transitional magma series. The rest eight samples fall on sub alkaline samples (tholeiitic magma series) on the AFM diagram of Irvine and Baragar (1971). see (Fig. 4.2B).

The samples are characterized by silica content (44.9-52.1 wt %) , high in MgO (4.29-16.35 wt. %), TiO₂ (0.79-2.03 wt. %), Fe₂O₃ (9.12-14.25wt. %), FeOt (8.1-12.7), CaO (8.51- 12.55 wt. %), total alkali Na₂O +K₂O (1.08-4.54wt. %) . LOI (0.1 to 2.02 wt. %); implies the samples are not altered. In terms of normative compositions, only one sample (**BS-13**)falls under the silica undersaturated (Alkali olivine basalt), characterizing by olivine and nepheline normative. Transitional and tholeiitic basalts (**BS-9** and **BS-12**) respectively grouped into silica saturated (olivine tholeiitic) having hypersthene and olivine normative. The rest samples are classified as silica oversaturated group (quartz tholeiitic) having quartz and hypersthene normative.



■ Alkaline Basalt ◆ Tholeiitic Dolerite ◆ Tholeiitic Basaltic andesite ▲ Tholeiitic Basalt ● Transitional Basalt

Figure 4.2) (A) Total alkali vs. silica diagram after (Le Bas et al., 1986), for the classification of volcanic rocks of the Birsheleko volcanic rocks (B) AFM diagram for volcanic rocks of Birsheleko from Irvine and Baragars (1971).

MgO is used as a fractionation index because it is more effective for the mafic system (Winter, 2014). The MgO contents of the samples are variable ranging from 4.29 to 16.35 wt. %. The highest MgO content is found from **BS-12**. Most of the value is concentrated below 6 wt. % (Fig.4.4) suggesting that their fractionated nature. Most of the major and trace element variation diagrams do not show a clear trend, due to the presence of mantle source heterogeneity between the transitional, tholeiitic, and alkaline. Most of the basaltic rocks have MgO that ranges from 4.29 and 6%. The values seem to be concentrate even though they show a trend. The tholeiitic transitional basaltic rocks display decrease in SiO₂, K₂O, TiO₂, and Na₂O with decreasing MgO contents. Whereas CaO, Al₂O₃, and FeO_t do not show well-defined trends i.e they are scattered.

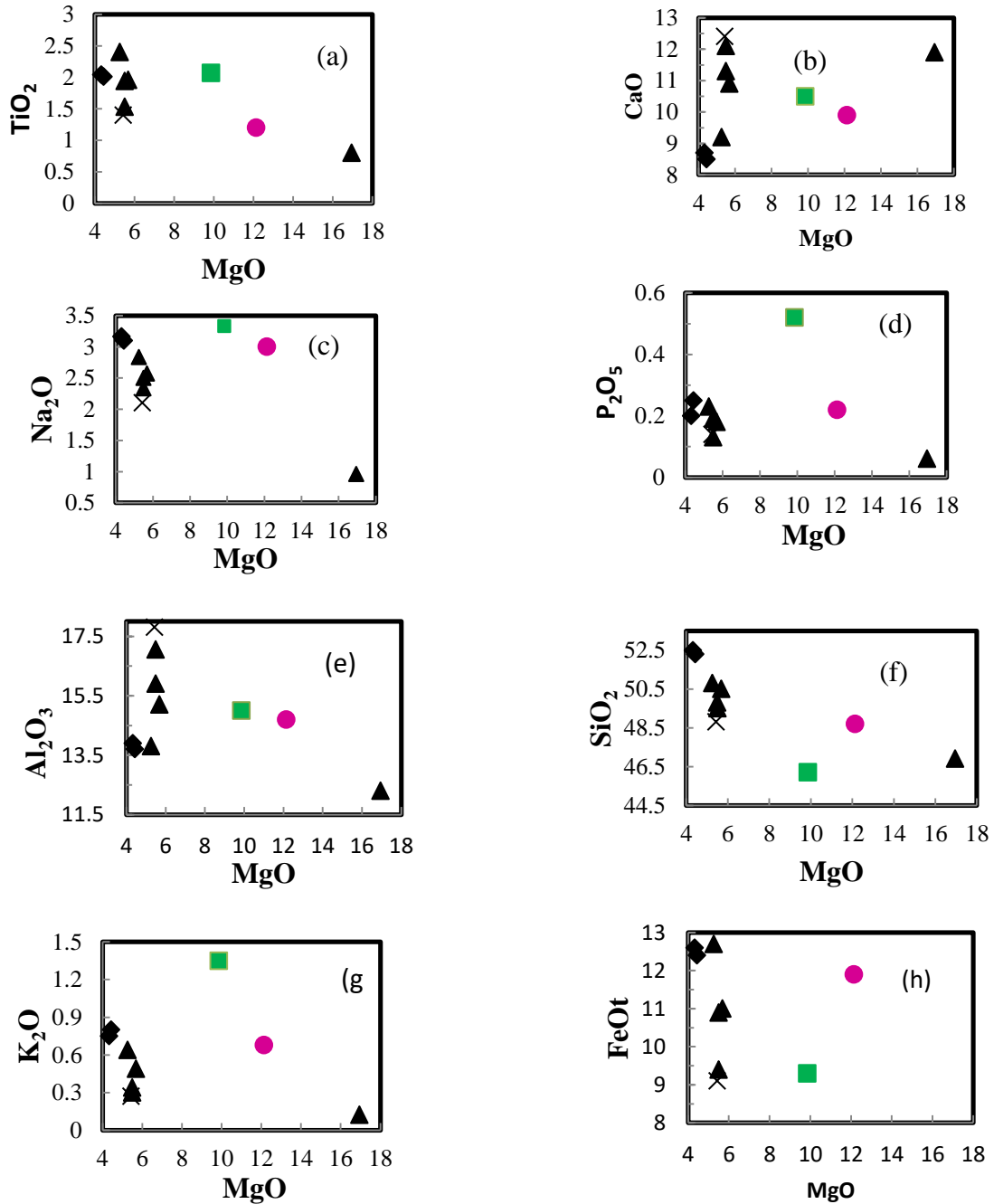


Figure 4.3) variation diagram for major oxides against magnesium oxide for Birsheleko volcanic and associated mafic dykes. The major element concentration is a volatile free base and expressed in wt. %.

4.3 Trace element geochemistry

All the volcanic rocks exhibit a wide range of trace element concentrations (Table 4.2). The concentration of compatible elements such as Cr varies from 1460 to 20 ppm, Ni from 569 to

19 ppm, V from 162ppm to 375 ppm, Cu from 62 to 149 ppm, and Sc from 22 to 35 ppm. Ni and Cr, exhibit a strong positive correlation with MgO. Co and V have a negative correlation with MgO; however, Cu and Sc have no clear trend.

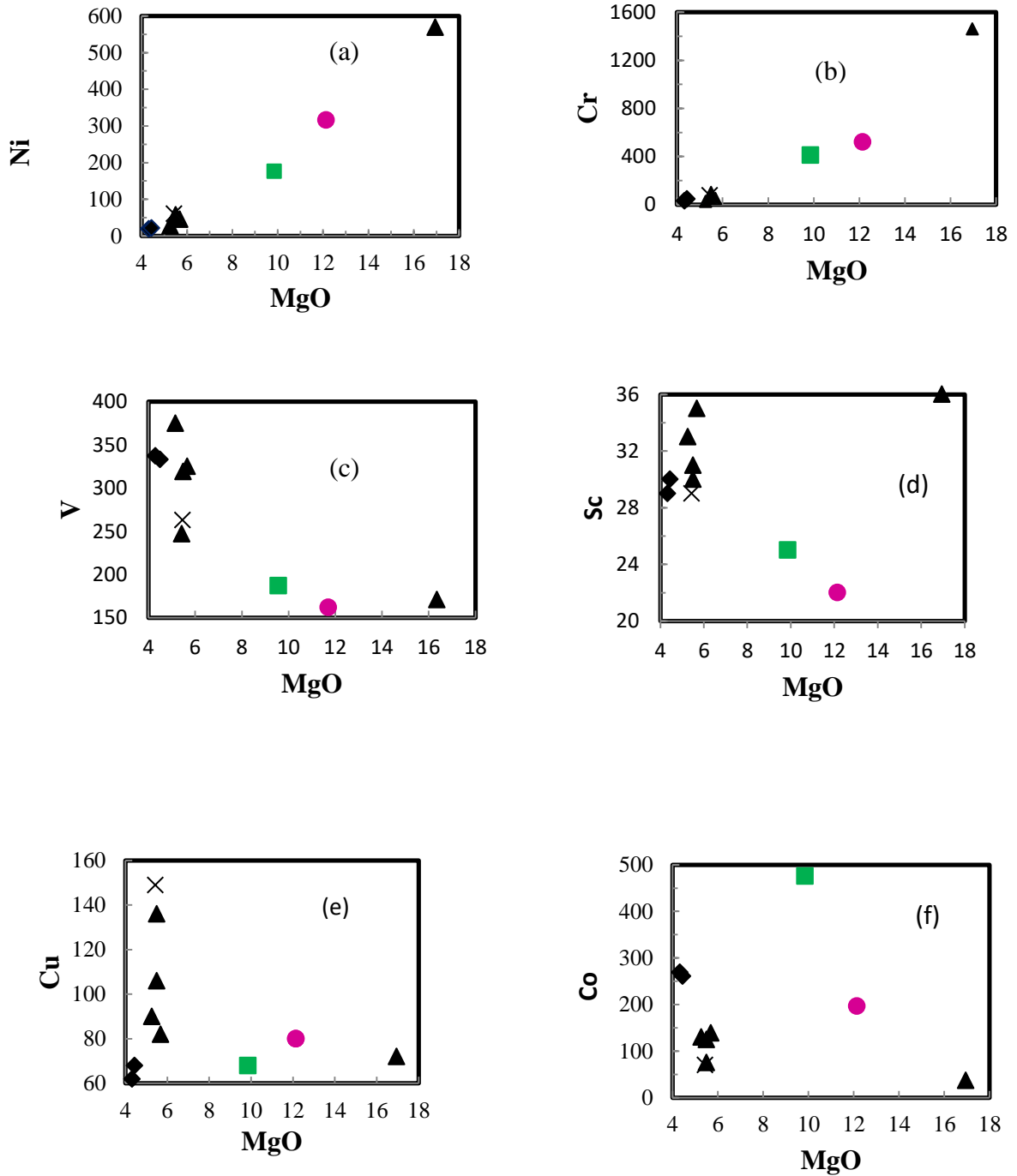


Figure 4.4) Variation diagram of compatible trace element vs. MgO. The unit for the concentration is in ppm for trace element and wt. % for the major element (MgO).

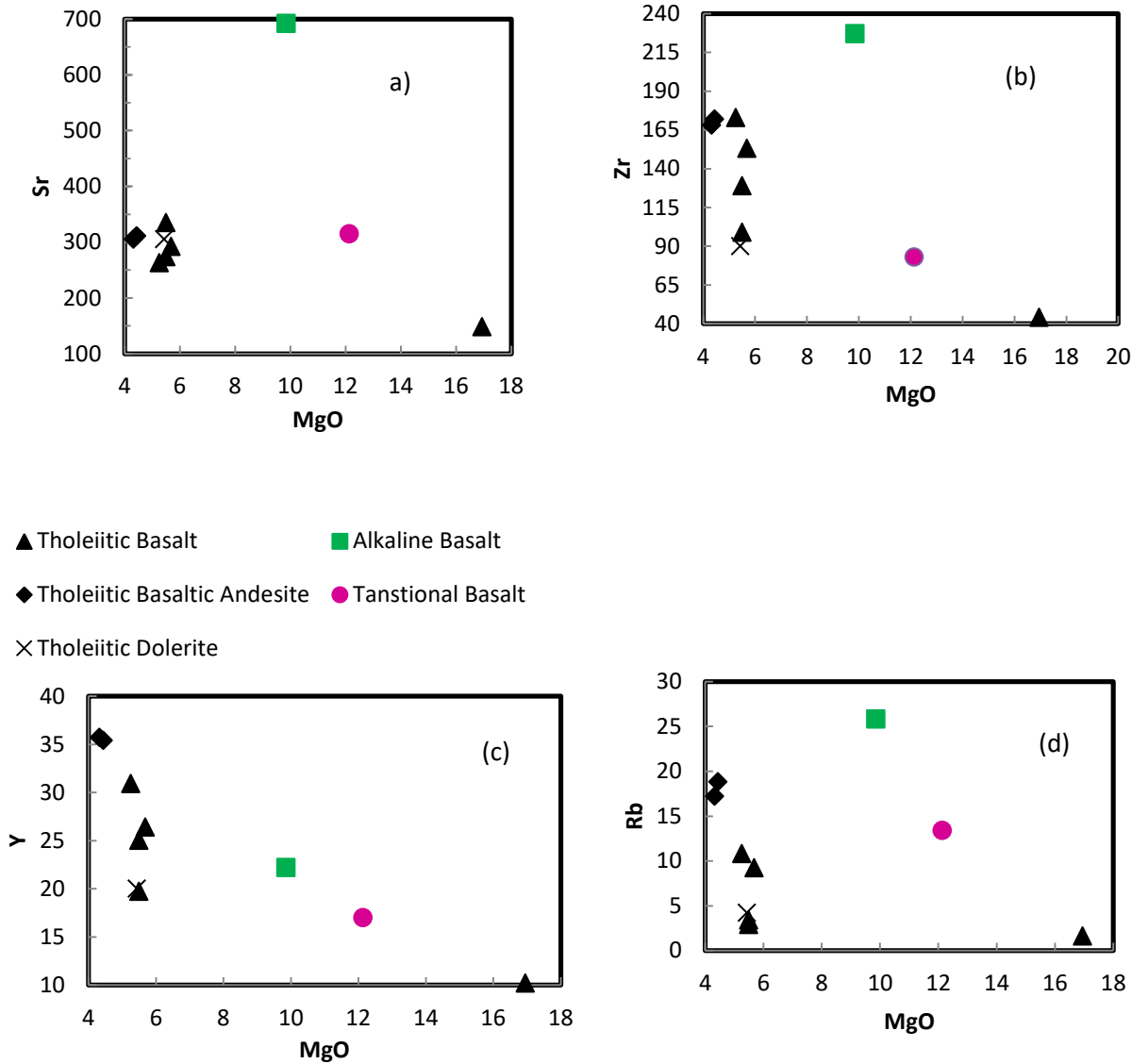


Figure 4.5) Variations diagram of incompatible trace elements Vs MgO (wt. %) for the volcanic rocks and associated mafic of the Birshaleko area from Northwestern Ethiopian plateau.

4.4 Rare earth element pattern

Rare Earth Elements are commonly immobile and did not affect by hydrothermal activity; hence, they play an important role in identifying the geochemical characteristic of the magma (Rollinson, 1993). Chondrite normalized rare earth element (REE) abundance for the volcanic rock is presented in (Fig.4.6). Furthermore, NMORB, E-MORB, and OIB are presented together for comparison. The studied samples are all light REE (LREE) enriched ($(Ce/Yb)_N = 2.08-4.32$) and slightly depleted HREE ($(Dy/Yb)_N = 1.25-1.54$) except one sample which is alkaline basalt (**BS-13**) (have $(Ce/Yb)_N = 9.72$, $(Dy/Yb)_N = 1.33$), where the subscript

N means Chondrite normalized. Two basaltic samples (**BS-13 and BS-9**) have a similar trend with that of OIB. The patterns of the REE show parallel to sub-parallel for all of the tholeiites (tholeiitic basalts, basaltic andesite, and dolerite) indicating they have similar mantle source. Sometimes the tholeiites cross with the alkaline and transitional basalt referring to the presence of mantle source heterogeneity.

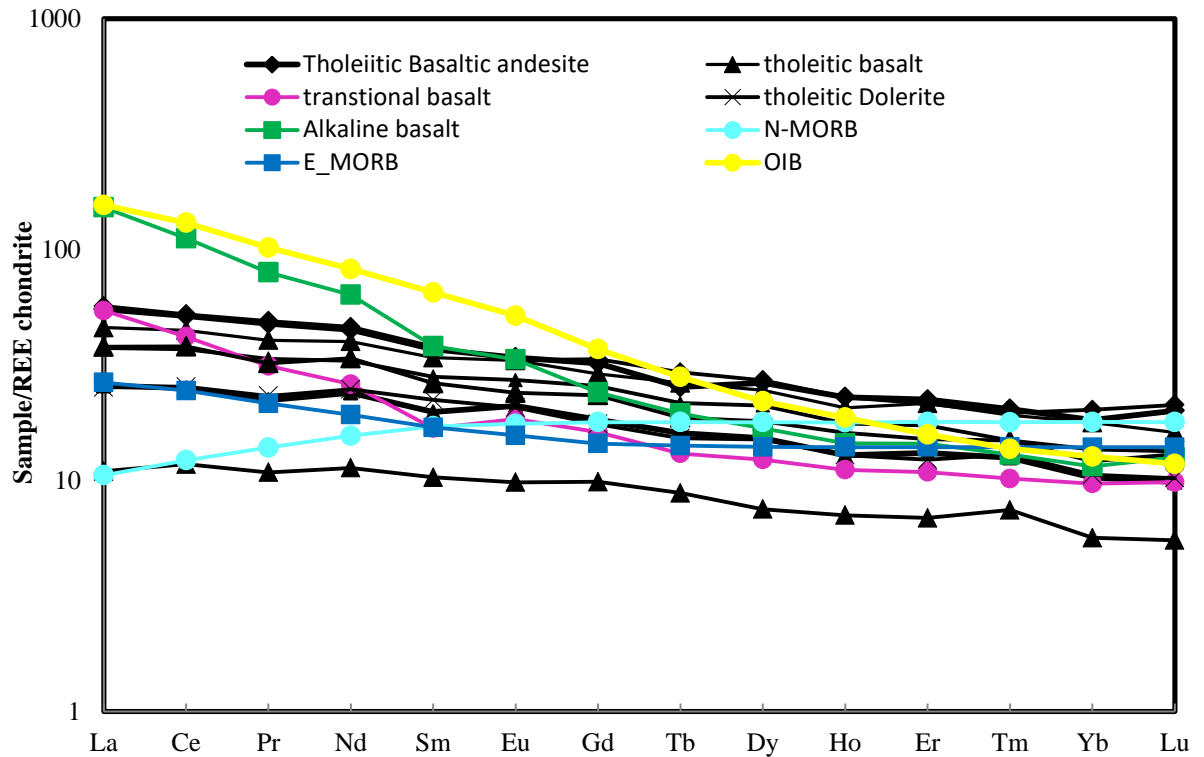


Figure 4.6) Chondrite normalized REE spider diagram of rocks from Birsheleko area. The concentration value of Normalizing values and OIB, E-MORB, and N-MORB data are from (Sun and McDonough, 1989).

The primitive mantle normalized multi-element variation patterns were plotted on (Fig.4.7). Thus, the samples are normalized to primitive mantle concentration values determined by Sun and McDonough (1989). The tholeiitic basalts and basaltic andesites show depletions in Rb, Th, Ce, Pr, P, and Nb and prominent peaks at Ba, K, Pb, U, and Sr. The transitional and alkaline basalts show enrichment in Pb, Sr, Nb, Ba. Depletion in Sm, Pr, and the positive anomaly is not observed at U and K. The rocks have almost similar and parallel patterns. The patterns are remarkably similar within the tholeiites (tholeiitic basalts, dolerite, and basaltic

andesites). But, sometimes display intersecting trace element patterns among the alkaline and tholeiites, implying that the basalts might not be genetically related.

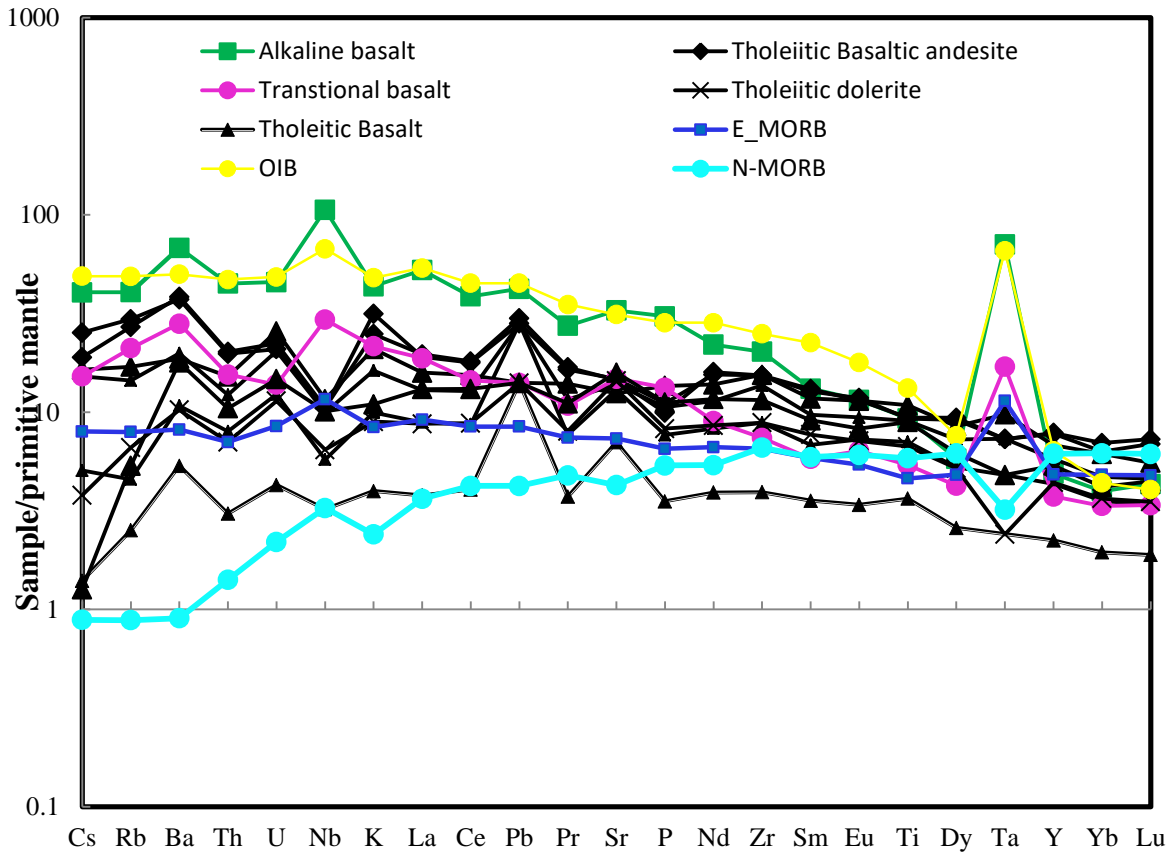


Figure 4.7) Primitive mantle normalized multi-element for volcanic rocks of the Birsheleko area. Normalizing values and OIB, E-MORB, and N-MORB data are from Sun and McDonough (1989).

The major and trace element compositions are used to evaluate whether the studied samples are genetically related or not. The Harker variation diagram, spider plot diagram, and again from their mantle source characterization clearly shown that the tholeiites namely the tholeiitic basalts, dolerite, and basaltic andesite dykes are genetically related and formed from the same mantle source. But the tholeiites are not genetically related to the alkaline and transitional basalts.

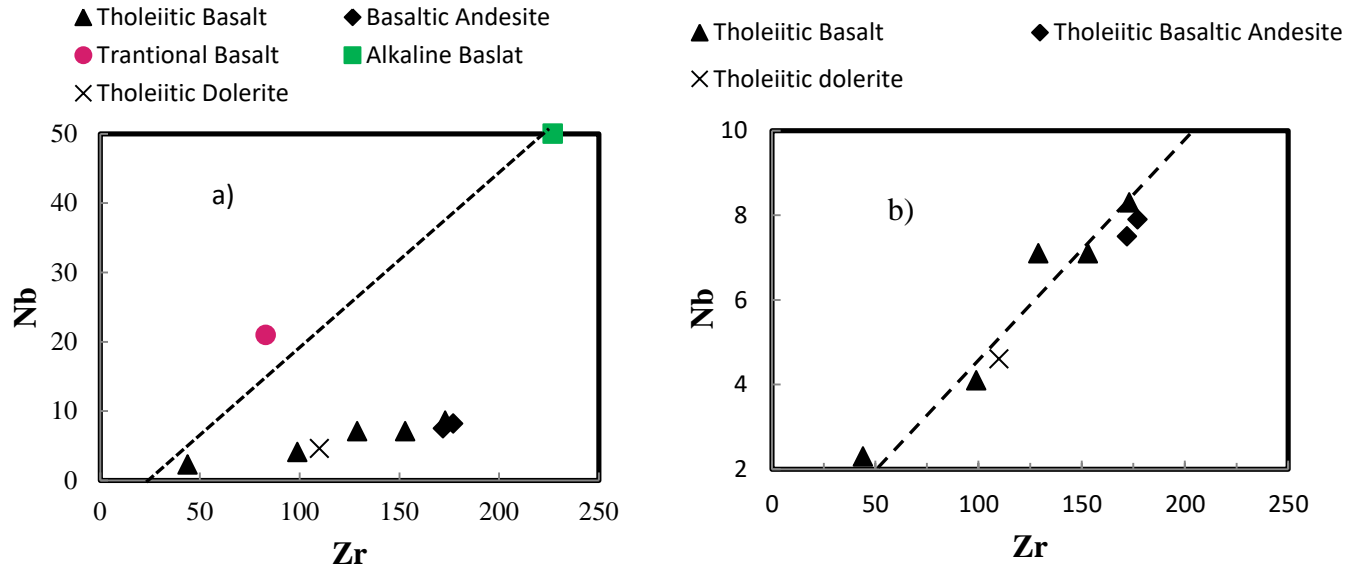


Figure 4.8) Nb vs. Zr plots to determine the genetic relationship between the tholeiites, alkaline, and transitional basalts. a) The alkaline and the transitional basalt showing the linear relationship, the tholeiites, alkaline, and transitional did not show a linear trend. b) Nb Vs. Zr plot to determine the genetic relationship between the tholeiitic basalts, tholeiitic dolerite, and tholeiitic basaltic andesite dykes showing linear relationship after (Hutchison et al., 2016).

In the study area, Basaltic andesite and Dolerite dykes are found. The samples taken from those dykes fall on tholeiitic magma series (**BS-4**, **BS-5**, and **BS-11**) i.e. the dykes are compositionally tholeiitic. From the primitive mantle normalized and Chondrite normalized spider diagrams (Figs 4.6 and 4.7) the tholeiitic dykes show a similar pattern with that of the tholeiitic basalts. From the Nb vs Zr diagram (Fig. 4.8b), a clear linear trend is observed between the tholeiitic basalt (country rock) and the tholeiitic basaltic andesite and tholeiitic dolerite (the dykes). This indicates the dykes are genetically related to the tholeiitic basalts. Besides, from the above diagram (Fig. 4.8: a) the alkaline and the transitional basalt showing linear relationships indicating they are genetically related. Again in Fig. 4.9a) the tholeiites (tholeiitic basalt, tholeiitic basaltic andesite, and tholeiitic dolerite) did not show a linear trend with the alkaline and transitional basalts. Indicating they are not genetically related.

CHAPTER FIVE

5. DISCUSSION

5.1 Fractional crystallization

Petrographically plagioclase, orthopyroxene, clinopyroxene, and olivine present as phenocryst, and Fe –Ti oxides like magnetite and ilmenite present as groundmass. Plagioclase, olivine, and pyroxenes present as groundmass in the transitional tholeiitic magmas (the samples except the alkaline one have such kind of property), indicate the occurrence of shallow level fractional crystallization. However, the alkaline magma has pyroxenes and some amount of olivine as phenocryst, but it does not have plagioclase at the phenocryst level (see Fig. 3.8). This could be interpreted that the alkaline basalt (**BS-13**) fractional crystallization occurred on a deeper level either in the lower crust or the mantle (Pik et al., 1998). The compositional variations from mafic to intermediate and felsic rocks are predominantly controlled by the fractional crystallization process (Chazot and Bertrand, 1995). Even though there is some kind of fractional crystallization observed, fractional crystallization is not dominant, and a major responsible process for the formation of the rocks. Inflected trends are also observed indicating the change in the fractionating phases (see Fig. 4.3 a, d, and g). Primitive mantle-normalized incompatible trace element spider diagrams (Fig. 4.7) show typical intraplate volcanic patterns with enrichment in incompatible elements.

The basaltic samples in the study area have Ni (19-316ppm) and Cr (20 -520ppm) as well MgO (4.29–11.7 wt. %). The values are low comparing to a primary magma that has Ni: > 400–500 ppm, MgO: 10–15 wt. % and, Cr: >1000 ppm (Frey et al., 1978; Hess, 1992). But, sample (**BS-12**, which is olivine phyric tholeiitic basalt have similar compositions with primary magma having MgO (16.35 wt %), Ni (569ppm), Cr (1460ppm). The basalts from the study area have undergone olivine and clinopyroxene fractionation. Negative correlations of SiO₂, FeO_t, Na₂O, and Al₂O₃ contents against MgO in tholeiitic samples (Fig. 4.3) support this inference because decreases in these element concentrations are expected during the fractionation of these minerals. So, all basaltic rocks of the study area except BS-12 were

derived from a differentiated primitive magma source. There is a scattering distribution between the tholeiitic, alkaline, and transitional samples.

The observed variation among the major oxide vs. MgO and compatible vs. MgO variation diagram (shown in Figs. 4.3 and 4.4), the slightly continuous decrease in FeO_t when plotted against MgO (Fig. 4.3) indicate fractionation of magnetite during the evolution of the magma. The fractionation of olivine is inferred from a decrease of Ni as MgO decreases. While the fractionation of clinopyroxene is characterized by a decrease of, Cr and Sc concentration as MgO increase.

5.2 Interaction with crustal materials

Mantle derived magmas can be modified by the assimilation of crustal materials during ascent to the surface through the crust with staying in magma chambers located at different crustal level processes. The contamination of the magma by crustal material has an impact upon incompatible trace element compositions (e.g., Rollinson, 1993; Furman, 2007; Wilson, 2007). Trace elements are useful to identify the possible involvement of crustal material during the emplacement of mafic magmas and ascent.

Ce/Pb, La/Ta ratios of mafic lavas are sensitive to contamination and well-defined for primary mantle-derived liquids (Ce/Pb ratio: 20 -30, Hofmann et al., 1986; La/Ta ratio <22 Hart et al., 1989). The basaltic rocks in the study area have a Ce/Pb ratio of 6.42–19.5 except two samples, which are alkaline and transitional (**BS-13**, and **BS-9**) have Ce/Pb ratio of 23, and 27.4 respectively. The La/Ta ratio of eight (8) samples ranges from 28–60 which is extremely huge except for **BS-9** and **BS-13**. Samples with code **BS-9** (18) and **BS-13** (12.44) are similar to primitive mantle i.e <22. Based on this most of the samples were affected by crustal contamination however, sample code **BS-9**(transitional basalt) and **BS-13** (alkaline basalt) are not affected by crustal contamination (see Fig. 5.2).

Besides, the

presence of Low Nb/La ratios (<1.0) in volcanic rocks is a good indicator of crustal contamination (Pik et al; Kieffer et al., 2004). Accordingly, the tholeiitic basaltic rocks in the study area have low values of the Nb/La ratio (0.55-0.88) that is (<1.0) in contrast, transitional and Alkaline basalts have Nb/La of 1.63 and 1.48. This shows that the tholeiites

(tholeiitic basalt, basaltic andesite, and dolerites) are affected by crustal material, however; the alkaline and transitional basalts are not affected by crustal contamination.

Furthermore, the presence of negative Nb and positive Pb and U anomalies in the primitive mantle normalized trace element patterns are good indicators for the existence of crustal contamination (Furman, 2007; Zhilong et al., 2013). Accordingly, the tholeiitic basaltic rocks have negative Nb, positive Uranium anomalies, and show Pb enrichment. However, the alkaline and transitional basalts have a positive Nb anomaly and don't show enrichment in U and Pb (Fig.4.7). These are a good indicator for tholeiitic to be crustally contaminated but, the transitional and alkaline basalts are not affected by crustal contamination.

5.3 Mantle source characteristics

Basaltic magma can be formed by partial melting of either the asthenospheric mantle or metasomatized lithospheric mantle, and by mixing of both (McDonough, 1990 and McKenzie and O'Nions, 1995). As stated by Smith et al., (1999) it is accepted that HFSE's such as Nb and Ta are depleted in the lithospheric mantle sources compared to the asthenosphere. From the primitive mantle normalized REE diagram, the tholeiites show depletion in Nb and Ta, but the alkaline and transitional basalts are enriched in Nb and Ta. Similarly, De Paolo and Daley (2000) suggest that the ratio of La/Nb is ~0.7 for an asthenospheric source and if the ratio is > 1, it indicates a lithospheric source. Consequently, the tholeiitic (basalts, dolerite, and basaltic andesite) have La/Nb (1.1-1.8) i.e >1, while the transitional basalt and the alkaline have 0.67 and 0.72 respectively. Therefore it is concluded that tholeiites (basalts, basaltic andesite, and dolerite) drive from the lithosphere whereas the transitional and the alkaline basalts are from the asthenosphere. The geochemical characteristics of the LT lavas are consistent with shallow level fractionation, dominated by plagioclase plus various amounts of olivine and clinopyroxene fractionation.

The trace element distribution patterns of the studied (alkaline and the transitional) rocks are similar to OIB, which probably represents basaltic melts from the enriched asthenosphere mantle source, often associated with an uprising mantle plume (Wilson, 1989). The geochemical data based on trace element variation of mafic rocks, which are alternating in the lithological sequence, suggest two different sources, a lithospheric mantle, and an asthenospheric mantle.

5.4 Degree of partial melting

The ratio of trace elements like Ba/Nb, La/Nb, increases as a degree of partial melting increases (Bougault et al., 1980). The studied tholeiitic samples have Ba/Nb (15.58-19.57), La/Nb (1.13-1.48). whereas the transitional and the alkaline samples have Ba/Nb (9.35 and 9.12), La/Nb (0.61 and 0.72) respectively. Besides $(La/Sm)_N$ is sensitive to the degree of partial melting, as the $(La/Sm)_N$ increases the degree of partial melting decreases (Dostal, 2019). As shown in the diagram (Fig. 5.1), the tholeiites (tholeiitic basalts, basaltic andesite, and dolerite) have low $(La/Sm)_N$ than that of the alkaline and the transitional basalts. From this, it is concluded that the alkaline basalts formed by a low degree of partial melting than the tholeiites. The transitional basalt is formed by an intermediate degree of partial melting. Besides, La/Lu ratios are helpful to estimate the degree of partial melting as La/Lu increases the degree of partial melting decreases (Feigenson et al., 1996). The tholeiites have La/Lu(18.25-26.5), the transitional and alkaline basalts have La/Lu (51.6 and 112.8) respectively.

Furthermore, a large degree of melting at lower pressure produces magma with hypersthene and quartz whereas, a small degree of partial melting at high pressure produces magma with normative nepheline (Depaolo and Dalley, 2000). From the CIPW norm, all the samples in this study area except **BS-13** has hypersthene and quartz normative, but **BS-13** is nepheline normative, so the tholeiitic samples are formed by a large degree of partial melting at low pressure, while the alkaline basalt is formed a small degree of partial melting at high pressure. The transitional basalts are formed by an intermediate degree of partial melting. Among the studied samples **BS-13**(Alkaline basalt), and **BS-12** (tholeiitic basalt) formed relatively at a low and high degree of partial melting respectively (Fig. 5.1). As a degree of partial melting increases, the concentration of incompatible trace elements decreases that is why a small amount of total trace elements is observed in the Chondrite normalized spider diagram of **BS-12** (Fig. 4.6).

Ratios of a low La/Yb ratio indicate the rocks are formed at low depth than those that have a greater La/Yb ratio (Ayalew et al., 2016). The tholeiitic samples of this study have a La/Yb ratio of 2.7 -4.4, the transitional and alkaline basalt samples have a La/ Yb ratio of 7 and 18.5 respectively. This means that the alkaline and the transitional basalts are formed at a

relatively greater depth than the tholeiitic (tholeiitic basalt, tholeiitic dolerite, and tholeiitic basaltic andesite) samples. By using Chondrite normalized $(Tb/Yb)_N$ ratio the relative depth in which the magmas formed can be determined. As $(Tb/Yb)_N$ ratio increases the depth in which the magma was formed also increases (Dostal et al., 2019). In the studied samples $(Tb/Yb)_N$ ratio the lowest value 1.3 (tholeiitic sample) and the highest value is 1.7 (alkaline basalt). Supporting the above idea that the alkaline magma formed at a greater depth than the tholeiites.

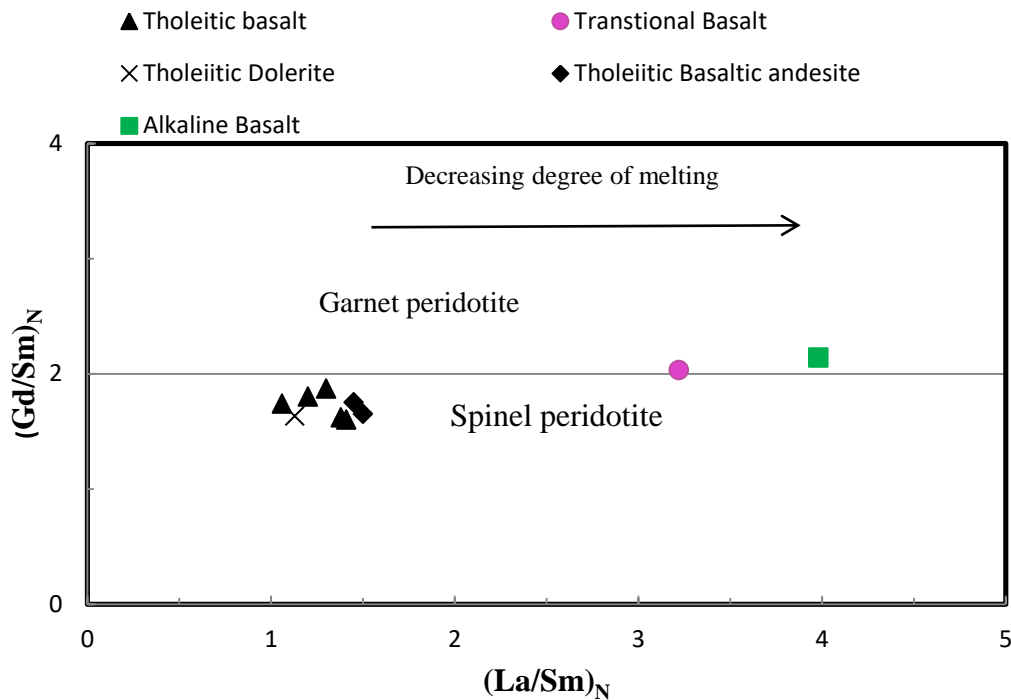


Figure 5.1 The $(La/Sm)_N$ Vs. $(Gd/Yb)_N$ diagram points to a spinel-bearing source for the tholeiites and the alkaline and the transitional basalts have a garnet-bearing source (after Alvaro et al.,2014). Normalization values of the Chondrite after Sun and McDonough (1989).

5.5 Comparison of the Birsheleko area basaltic rocks with the Ethiopian continental flood basalts

The Birsheleko area is mainly covered by basaltic rock. The bimodality nature of Ethiopian large igneous provinces has been discussed over by several researchers (e.g., Ayalew et al., 2002; Peccerillo et al., 2003; 2007; Rooney et al., 2017), the Birsheleko area does not have felsic volcanic rocks. Among the collected basaltic samples the two samples have similar

characteristics with alkaline and the rest eight samples (basaltic andesites, basalt, and dolerite samples) overlay with the tholeiitic field. TAS and AFM diagrams (Fig. 4.2) reveal that the presence of mafic and intermediate lavas. As well as the rocks grouped into transitional, alkaline, and tholeiitic series.

Three magma types namely: low Ti group (LT) and high-Ti groups (HT1 and HT2) and magmas are spatially distributed on the Ethiopian continental flood basalt. The LT suite exhibits high SiO₂ (47-51%), low TiO₂ (1-2.6 wt. %) and low Fe₂O₃ (10.5-14.8), CaO/Al₂O₃ (0.4-0.75), Nb/La (0.55-0.85). In contrast, the HT2 suite exhibits low SiO₂ (44-48.3%), high TiO₂ (2.6-5 wt. %), Fe₂O₃ (13.1-14.7), CaO/Al₂O₃ (0.9-1.43), Nb/La (1.1-1.4). The HT1 groups show intermediate characteristics between the LT and HT2 (Pik et al., 1998).

Accordingly, the tholeiites (the tholeiitic basalt, tholeiitic basaltic andesite, and tholeiitic dolerite) of this study have low TiO₂ (1.53-2 wt. %) and SiO₂ (45.3-49.9%), Fe₂O₃ (13.1-14.7), CaO/Al₂O₃ (0.7-0.96), and Nb/La (0.6-0.8). The transitional and alkaline basalts have TiO₂ (2.07 and 1.17 wt. %) and SiO₂ (44.9 and 47%), Fe₂O₃ (10.5 and 14.2), CaO/Al₂O₃ (0.7 and 0.6), and Nb/La (1.4 and 1.6). Based on the above classification the tholeiitic basalts of this study are classified under the LT group; however, the alkaline and the transitional basalts are grouped as HT1. Besides, in the primitive mantle normalized diagram, the tholeiitic basalts and dolerite samples show depletion in Nb, Ta, and Th and enrichment in Pb and Ba (Fig. 4.7). That is also observed in LT of Pik et al. (1999). Furthermore, in the Nb/Y versus Ti/Y diagram the tholeiitic basalt and dolerite fall in the LT group (Fig. 5.2). The alkaline and the transitional basalt fall in the HT1 group. This confirms that the studied samples show nearly similar geochemical character to previously reported basaltic rocks from Northwestern Ethiopia Plateau and MER (Pik et al., 1998, Kieffer et al., 2004; Beccaluva et al., 2009 and Hagos et al., 2016).

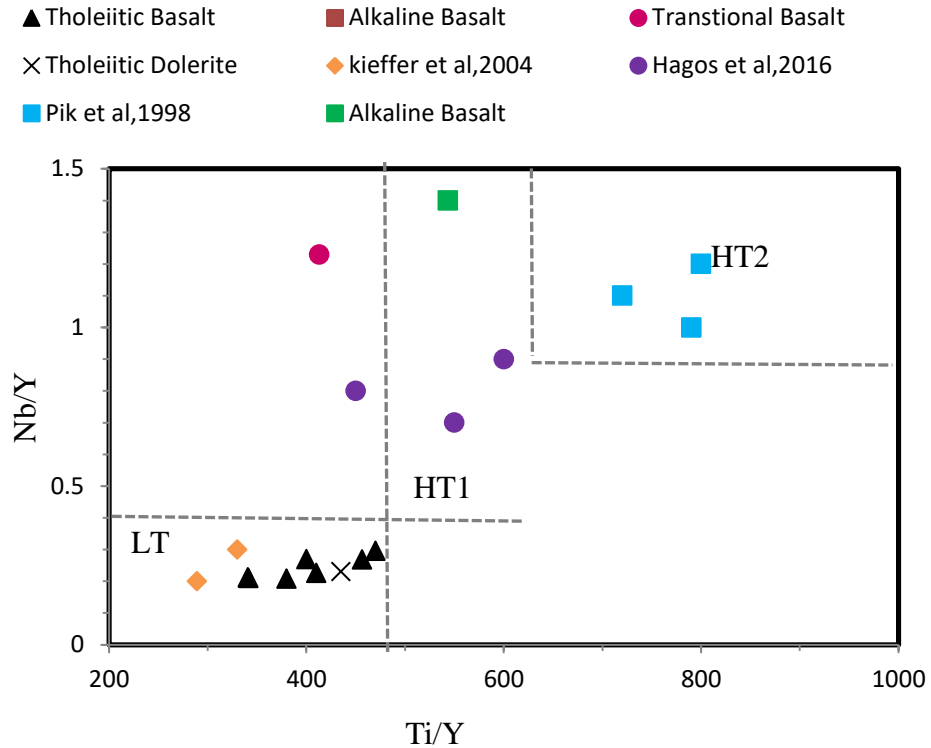


Figure 5. 2 Nb/Y versus Ti/Y diagram for Birsheleko area volcanic rocks and associated mafic dykes after (Pik et al., 1998).

The petrographic description of LT basalts from the Birsheleko area confirmed the (Pik et al., 1998; Meshesha and Shinjo, 2004; 2007) petrographically characterization of plateau basalts as to glomeroporphyritic with rarely aphyric textures consisting of plagioclase, clinopyroxene, and olivine phenocrysts. Sub ophitic nature with aggregates of clinopyroxene phenocryst led them to have a tholeiitic affinity. In the meantime, these LT basalts show the olivine, quartz, and hypersthene normative. The Tholeiitic samples from this study namely the tholeiitic basalt, tholeiitic Basaltic Andesite, and Tholeiitic Dolerite are affected by crustal contamination (as shown in Fig. 5.3). However, two samples which are alkaline and transitional basalts are not affected by crustal contamination. Samples from the Northwestern Ethiopian plateau (from Bure, Limalimo, and Zarema), Northern Afar depression (MER) were used for comparison purposes. In detail, two basaltic rock samples from Lima limo and one sample from the Zarema section (Kieffer et al., 2004) have a low Ce/Pb ratio (10,10.6, and 13.4). Among the seven samples from Bure volcanic rocks (Meshesha and Shinjo, 2004) two alkaline basalts have Ce/Pb of (23.6 and 24); however, the rest five tholeiitic -transitional basalts have a Ce/Pb ratio of (6 -17.5). This may be due to a series of involvement of crustal

materials during their evolutions respectively. Among four basaltic rocks from the Northern Afar depression (Hagos et al., 2016) three samples have a high Ce/Pb ratio (23.6-29) and fall in the mantle value, which is evidence of no crustal involvement. Only one sample falls in the crustal region with a Ce/Pb ratio (15.6) which encourages the involvement of crustal materials during its evolution. Only two basaltic rocks (the transitional and the alkaline basalts) in this study area have Ce/Pb ratios value of (25.7, and 23.3), which is in the range of mantle value but the rest samples fall on the region of crustal contamination.

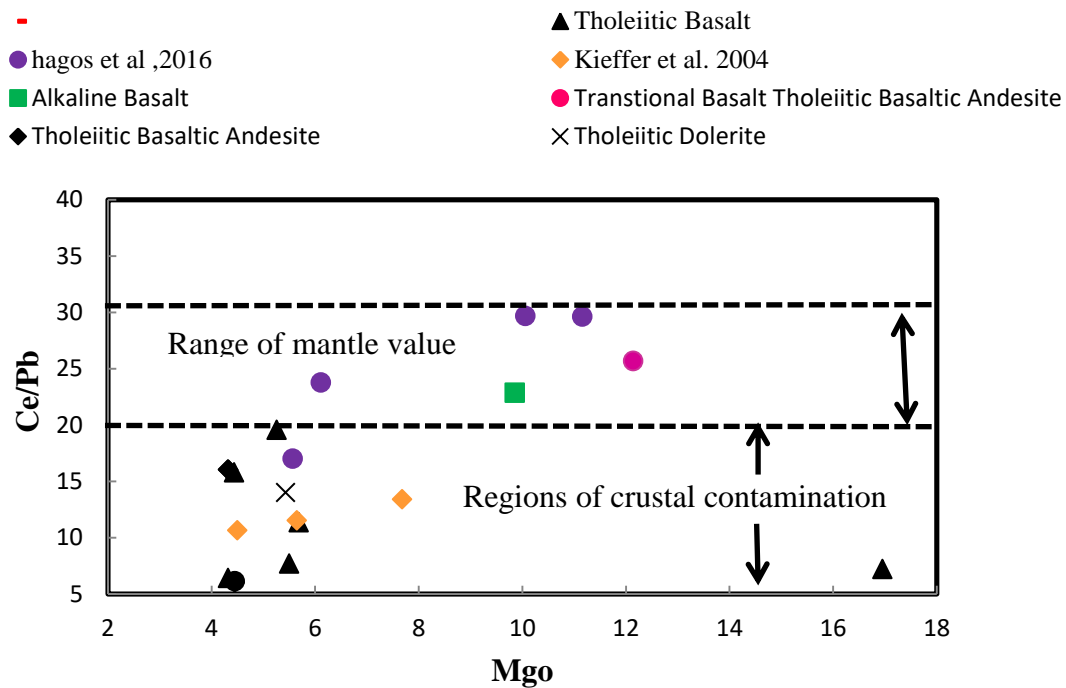


Figure 5.3) Ce/Pb vs. MgO (wt. %) after Hofmann et al., (1986) for the Birsheleko volcanic rocks showing crustal contamination effect. Data for the volcanic rocks from Hagos et al., 2016 and Kieffer et al., 2004 have been included for comparison.

Generally from the above discussion, it can be summarized that the tholeiitic (dolerite, basaltic andesites, and basalts) of the Birsheleko area are crustally contaminated. However, alkaline and transitional basalts are not contaminated. It is supported by the work of (Pik et al., 1998; Baker et al., 2000; Kieffer et al., 2004; Meshesha and Shinjo, 2004; 2007). Like the tholeiitic basalts in this study area, the tholeiitic basalts of Lima limo region (Pik et al.,

1998), Bure (Meshesha and Shinjo, 2004; 2007), Semien shield (Kieffer et al., 2004), Yemen (Baker et al., 2000) are also crustally contaminated, but the alkaline (Guna) is not.

The studied tholeiitic samples are formed by the melting of spinel bearing mantle source and the alkaline and transitional basalts are formed by the melting of garnet-bearing mantle source. Like ways the LT and HT1 samples that were taken for comparison from the Northwestern Ethiopian plateau (Pik et al., 1999 and Kieffer et al, 2004) display similar characteristics that they are formed by melting of spinel mantle source and garnet mantle source respectively. Besides, the tholeiites of the Birsheleko area and the LT basalts of Northwestern Ethiopia are crustal contaminated. However, the Birsheleko alkaline and transitional basalts and HT1 basalts from the Northwestern Ethiopian plateau are not.

Therefore, it can be concluded that there is a similarity in the degree of partial melting, source composition, and melting depth between Birsheleko volcanic rocks and associated mafic dykes with the basaltic rocks from the Northwestern Ethiopian plateau. Even though the MER basalts have trace element characteristics similar to OIB basalts are derived by a moderate degree of partial melting from spinel bearing peridotite (Ayalew et al., 2016) They are different in Petrogenesis from the Birsheleko area basalts and flood basalts of the Northwestern Ethiopian plateau.

CHAPTER SIX

6. CONCLUSION AND RECOMMENDATION

6.1 Conclusion

Based on the field observations, petrographic descriptions, and whole-rock geochemistry the following conclusions have been drawn. The major lithological units identified in the studied area are porphyritic basalt, aphanitic basalt, basaltic andesite, dolerite, vesicular basalt, thin scoriaceous basaltic flow, vesicular basalt, and scoria cones. The studied samples show aphyric and porphyritic texture under the petrographic microscope investigation. Plagioclase, pyroxenes (Orthopyroxene and clinopyroxene) \pm olivine present as a phenocryst. The groundmass consisting of similar mineral assemblage as the phenocryst plus opaque minerals. Based on modal analysis carried out plagioclase phyric basalt and dolerites, olivine phyric basalt, pyroxene phyric basalt, aphyric trachy flow basaltic andesite, and aphyric trachy flow basalt present. The geochemical data shows the presence of mafic and intermediate rocks. Most of the studied samples are sub alkaline (tholeiitic), but two samples fall in transitional and alkaline groups. The tholeiitic basalts are grouped as LT when the alkaline and transitional basalts are grouped as HT1. The major and trace element variation diagram, trace element modeling (Nb versus Zr variation diagram), multi-element variation diagram shows the presence of mantle source heterogeneity between the tholeiitic, alkaline, and transitional samples. The dykes (the tholeiitic dolerite and tholeiitic basaltic andesite) are genetically related to the tholeiitic basalt. The tholeiitic basalts and tholeiitic basaltic andesite rocks are related to each other by some kind of fractional crystallization. They are also formed are formed by a high degree of melting of the lithosphere at low pressure. Besides, the transitional and alkaline is samples are and formed by a low degree of melting of the asthenosphere at high pressure and greater depth than the tholeiites; however, they are not genetically related to the tholeiites. The tholeiitic samples (tholeiitic basalt, tholeiitic dolerite, and tholeiitic basaltic andesite) are affected by crustal contamination. On the contrary, the alkaline and the transitional basalts are not.

6.2 Recommendation

The present study has reached the above conclusions based on field observation, petrographic description, and geochemical data interpretation. However, to fully understand the magmatic evolution of the Birsheleko area volcanic rocks and associated mafic dykes, it needs further investigation. Therefore the following studies are recommended for future works such as:

- ❖ Mineral chemistry analysis for phenocryst, microphenocryst phases, and groundmass level is required to know the mineral composition of the volcanic rocks and associated mafic dykes qualitatively.
- ❖ Isotopic geochemistry analysis is recommended to know which part of the crust is responsible for the existence of crustal contaminated tholeiitic basalts.
- ❖ A detailed Geothermobarometry study of minerals is suggested to determine the pressure and temperature condition in which the rocks formed.

References

- Abbate, E., & Sagri, M. (1980). Volcanites of Ethiopian and Somali Plateaus and major tectonic lines. *Atti Convegni Lincei*, 47, pp.219-227.
- Alemayehu, T. (2006). Groundwater occurrence in Ethiopia. Addis Ababa University, Addis Ababa, Ethiopia.
- ALS, (2017). Analytical Testing Services Manual, 33p.
- Álvaro, J. J., Pouclet, A., Ezzouhairi, H., Soulimani, A., Bouougri, E. H., Imaz, A. G., & Fekkak, A. (2014). Early Neoproterozoic rift-related magmatism in the Anti-Atlas margin of the West African craton, Morocco. *Precambrian Research*, 255, 433-442.
- Ayalew, D., & Yirgu, G. (2003). Crustal contribution to the genesis of Ethiopian plateau rhyolitic ignimbrites: basalt and rhyolite geochemical provinciality. *Journal of the Geological Society*, 160(1), 47-56.
- Ayalew, D., Barbey, P., Marty, B., Reisberg, L., Yirgu, G., & Pik, R. (2002). Source, genesis, and timing of giant ignimbrite deposits associated with Ethiopian continental flood basalts. *Geochimica et Cosmochimica Acta* .66, 1429–1448.
- Ayalew, D., Jung, S., Romer, R. L., Kersten, F., Pfänder, J. A., & Garbe-Schönberg, D. (2016). Petrogenesis and origin of modern Ethiopian rift basalts: Constraints from isotope and trace element geochemistry. *Lithos*, 258, 1-14
- Baker, J.A., Macpherson, C.G., Menzies, M.A., Thirlwall, M.F., Al-Kadasi, M., and Matthey, D.P. (2000). Resolving crustal and mantle contributions to continental flood volcanism, Yemen; constraints from mineral oxygen isotope data. *Journal of Petrology*, 41(12), pp.1805-1820.
- Beccaluva, L., Bianchini, G., Natali, C., & Siena, F. (2009). Continental flood basalts and mantle plumes: a case study of the Northern Ethiopian Plateau. *Journal of Petrology*, 50(7),1377-1403.
- Best, M.G. (2003). Igneous and metamorphic petrology. *Blackwell publishing company*.
- Bougault, H., Joron, J.L., and Treuil, M., 1980. The primordial chondritic nature and largescale heterogeneities in the mantle: evidence from high and low partition coefficient elements in oceanic basalts. *Phil. Trans. R. Soc. Lond. A*, 297(1431), pp.203–213.

- Chazot, G., & Bertrand, H. (1993). Mantle sources and magma-continental crust interactions during early Red Sea-Gulf of Aden rifting in southern Yemen: Elemental and Sr, Nd, Pb isotope evidence. *Journal of Geophysical Research: Solid Earth*, 98(B2), 1819-1835.
- Cox K.G., Bell, J.D., & Pankhurst, R.J. (1979). The Interpretation of Igneous Rocks. *George Allen and Unwin*, London, 450p.
- DePaolo, D. J., & Daley, E. E. (2000). Neodymium isotopes in basalts of the southwest basin and range and lithospheric thinning during continental extension. *Chemical Geology*, 169(1-2), 157-185.
- Dercq, M., Arndt, N., Lapierre, H., & Yirgu, G. (2001). Les pitons volcaniques d'Ethiopie sont les conduits d'alimentation des trachytes des volcans boucliers. *Comptes Rendus de l'Académie des Sciences-Series IIA-Earth and Planetary Science*, 332(10), 609-615.
- Desta, M. T., Ayalew, D., Ishiwatari, A., Arai, S., & Tamura, A. (2014). Ferropicrite from the Lalibela area in the Ethiopian large igneous province. *Journal of Mineralogical and Petrological Sciences*, 109(4), 191-207.
- Desta, M. T., Ishiwatari, A., Machi, S., Arai, S., Tamura, A., Ledneva, G. V., ... & Bazylev, B. A. (2015). Petrogenesis of Triassic gabbroic and basaltic rocks from Chukotka, NE Russia: Eastern end of the 'arc-type' Siberian LIP?. *Journal of Mineralogical and Petrological Sciences*, 110(6), 249-275.
- Dostal, J., Keppie, J.D., & Church, B.N. (2019). Generation of Eocene volcanic rocks from the Cordilleran arc of south-central British Columbia (Canada) during subduction of the Farallon and Resurrection plates and Yellowstone oceanic plateau. *Geological Journal*, 54(1), pp.590-604.
- Feigenson, M. D., Patino, L. C., & Carr, M. J. (1996). Constraints on partial melting imposed by rare earth element variations in Mauna Kea basalts. *Journal of Geophysical Research: Solid Earth*, 101(B5), 11815-11829.
- Frey, F. A., Green, D. H., & Roy, S. D. (1978). Integrated models of basalt Petrogenesis: a study of quartz tholeiites to olivine melilitites from southeastern Australia utilizing geochemical and experimental petrological data. *Journal of petrology*, 19(3), 463-513.

- Furman, T. (2007). Geochemistry of East African Rift basalts: an overview. *Journal of African Earth Sciences*, 48(2-3), 147-160.
- George, R., Rogers, N., & Kelley, S. (1998). Earliest magmatism in Ethiopia: evidence for two mantle plumes in one flood basalt province. *Geology* **26**, 923-926.
- Hagos, M., Koeberl, C., & de Vries, B. V. W. (2016). The Quaternary volcanic rocks of the northern Afar Depression (northern Ethiopia): Perspectives on petrology, geochemistry, and tectonics. *Journal of African Earth Sciences*, 117, 29-47.
- Hart, W. K., WoldeGabriel, G., Walter, R. C., & Mertzman, S. A. (1989). Basaltic volcanism in Ethiopia: constraints on continental rifting and mantle interactions. *Journal of Geophysical Research: Solid Earth*, 94(B6), 7731-7748.
- Hess, P. C. (1992). Phase equilibria constraints on the origin of ocean floor basalts. *GMS*, 71, 67-102.
- Hofmann, A.W., Jochum, K.P., Seufert, M., & White, W.M. (1986). Nb and Pb in oceanic basalts: new constraints on mantle evolution. *Earth and Planetary science Letters*, 79(1-2), pp.33-45.
- Hofmann, C., Courtillot, V., Feraud, G., Rochette, P., Yirgu, G., Ketefo, E., & Pik, R. (1997). Timing of the Ethiopian flood basalt event and implications for plume birth and global change. *Nature*, 389(6653), 838-841.
- Huss, G.R., & McSween Jr, H.Y. (2010). *Cosmochemistry*. Cambridge University Press.
- Hutchison, W., Pyle, D.M., Mather, T.A., Yirgu, G., Biggs, J., Cohen, B.E., Barfod, D.N., Lewi, E. (2016). The eruptive history and magmatic evolution of Aluto volcano: new insights into silicic peralkaline volcanism in the Ethiopian rift. *J. Volcanol. Geoth. Res.* 328, 9–33
- Irvine, T. N. J., & Baragar, W. R. A. (1971). A guide to the chemical classification of the common volcanic rocks. *Canadian journal of earth sciences*, 8(5), 523-548.
- Kieffer, B., Arndt, N., Lapierre, H., Bastien, F., Bosch, D., Pecher, A., & Keller, F. (2004). Flood and shield basalts from Ethiopia: magmas from the African super swell. *Journal of Petrology*, 45(4), 793-834.
- Lafleche, M. R., Dupuy, C., & Bougault, H. (1992). Geochemistry and petrogenesis of Archean mafic volcanic rocks of the southern Abitibi Belt, Québec. *Precambrian Research*, 57(3-4), 207-241.

- Le Bas, M. J., Le Maitre, R., Streckeisen, A., & Zanettin, B. (1986). A chemical classification of volcanic rocks based on the total alkali-silica diagram. *Journal of Petrology* 27(3):745-750.
- McDonough, W. S. (1990). Constraints on the composition of the continental lithospheric mantle. *Earth and Planetary Science Letters*, 101(1), 1-18.
- McKenzie, D. A. N., & O'NIONS, R. K. (1995). The source regions of ocean island basalts. *Journal of petrology*, 36(1), 133-159.
- Merla, G., Abbate, E., Azzaroli, A., Bruni, P., Caunti, P., Fazzuoli, M., Sagri, M., & Tacconi, P. (1979). Geological map of Ethiopia and Somalia (1973):1:2,000,000. Comment with major landforms, 2-98.
- Meshesha, A. D., & Shinjo, R. (2004). Petrochemical evidence for the diversity of magma compositions at the northwestern Ethiopian volcanic province. *Bulletin of the Faculty of Science, University of the Ryukyus*, 78, 251-266.
- Meshesha, D., & Shinjo, R. (2007). Crustal contamination and diversity of magma sources in the northwestern Ethiopian volcanic province. *Journal of Mineralogical and Petrological Sciences*, 102(5), 272-290.
- Mohr, P. (1983). Ethiopian flood basalt province. *Nature* 303, 577-584.
- Mohr, P. A. (1971). Ethiopian rift and plateaus: some volcanic petrochemical differences. *Journal of Geophysical Research*, 76(8), 1967-1984.
- Mohr, P., & Zanettin, B. (1988). The Ethiopian flood basalt province. In *Continental flood basalts* (pp. 63-110). *Springer*, Dordrecht.
- Mohr, P., & Zanettin, B. (1988). The Ethiopian flood basalt province. In *Continental flood basalts* (pp. 63-110). *Springer*, Dordrecht.
- Pearce, J. A. (1982). Trace element characteristics of lavas from destructive plate boundaries. *Andesites*, 8, 525-548.
- Peccerillo, A., Barberio, M. R., Yirgu, G., Ayalew, D., Barbieri, M. W. U. T. W., & Wu, T. W. (2003). Relationships between mafic and peralkaline silicic magmatism in continental rift settings: a petrological, geochemical, and isotopic study of the Gedemsa volcano, central Ethiopian rift. *Journal of Petrology*, 44(11), 2003-2032.
- Peccerillo, A., Donati, C., Santo, A. P., Orlando, A., Yirgu, G., & Ayalew, D. (2007). Petrogenesis of silicic peralkaline rocks in the Ethiopian rift: geochemical evidence and volcanological implications. *Journal of African Earth Sciences*, 48(2), 161-173

- Pik, R., Deniel, C., Coulon, C., Yirgu, G., & Marty, B. (1999). Isotopic and trace element signatures of Ethiopian flood basalts: evidence for plume–lithosphere interactions. *Geochimica et Cosmochimica Acta*, 63(15), 2263-2279.
- Pik, R., Deniel, C., Coulon, C., Yirgu, G., Hofmann, C., & Ayalew, D. (1998). The northwestern Ethiopian Plateau flood basalts: classification and spatial distribution of magma types. *Journal of Volcanology and Geothermal Research*, 81(1-2), 91-111.
- Rollinson, H. R. (1993). A terrane interpretation of the Archaean Limpopo Belt. *Geological Magazine*, 130(6), 755-765
- Rooney, T. O. (2017). The Cenozoic magmatism of East-Africa: Part I-flood basalts and pulsed. *Lithos*, **286**: 264-301.
- Singh, A. K., & Singh, R. B. (2012). Petrogenetic evolution of the felsic and mafic volcanic suite in the Siang window of Eastern Himalaya, Northeast India. *Geoscience Frontiers*, 3(5),
- Smith, E. I., Sanchez, A., Walker, J. D., & Wang, K. (1999). Geochemistry of mafic magmas in the Hurricane Volcanic field, Utah: implications for small-and large-scale chemical variability of the lithospheric mantle. *The Journal of geology*, 107(4), 433-448.
- Sun, S. S., & McDonough, W. F. (1989). Chemical and isotopic systematics of oceanic basalts: implications for mantle composition and processes. *Geological Society, London, Special Publications*, 42(1), 313-345.
- Tefera M., Tadiwos C. & Workineh H. (1996). Explanation of the Geological Map of the northern Main Ethiopian Rift: the birth of a triple junction. *Earth and Planetary Science Letters*, 224: 213–228
- Tsige, L. (2008). Geology of Bure Map Sheet (NC37-5). Memoir No. 18. Geological Survey of Ethiopia. 86 pp. *Unpublished report*.
- Whitney, D. L., & Evans, B. W. (2010). Abbreviations for names of rock-forming minerals. *American mineralogist*, 95(1), 185-187.
- Wilson, B. (2007). Igneous petrogenesis a global tectonic approach.
- Wilson, M. 1989. Igneous Petrogenesis. Unwin Hyman, London, 446 p.
- Winter, J.(2014).Principles of igneous and metamorphic petrology.Pearson edition.
- Zhang, X., Zhang, H., Tang, Y., Wilde, S.A., & Hu, Z. (2008). Geochemistry of Permian bimodal volcanic rocks from central Inner Mongolia, North China: implication for

tectonic setting and Phanerozoic continental growth in Central Asian Orogenic Belt.
Chemical Geology, 249(3-4),pp.262-281.

Zhilong, J., Huang, Z., Luo, T., Qian, Z., & Zhang, Y. (2013). Geochemistry and petrogenesis of Late Ladinian OIB-like basalts from Tabai, Yunnan Province, China. *Chinese Journal of Geochemistry*, 32(4), pp.337-346.-590.

Appendix

Petrographic description

Sample code; BS-7 (Tholeiitic)					
Minerals	Modal proportion (%)	Phenocryst maximum grain size (mm)	Phenocryst maximum grain shape	Texture	Rock name
Plagioclase	20	1mm	Subhedral-Euhedral	Plag phyric Or porphyritic	Plag phyric basalt
Groundmass of: plagioclase, and opaque minerals	80				

Sample code: BS-8 and Bs-3 (tholeiitic)					
Minerals	Modal proportion (%)	Phenocryst maximum grain size (mm)	Phenocryst maximum grain shape	Texture	Rock name
Plagioclase	1-2	0.2mm		Aphyric	Aphyric trachy flow basalt
Groundmass of: plagioclase, and opaque minerals	98-99				

Sample code: BS-13 (Alkaline)					
Minerals	Modal proportion (%)	Phenocryst maximum grain size (mm)	Phenocryst maximum grain shape	Texture	Rock name
pyroxenes	30	1mm	Euhedral	Pyroxene -phyric	Pyroxene –phyric Basalt
Olivine	5				
The groundmass of plagioclase, olivine .clinopyroxene, orthopyroxene, and other opaque minerals	65				

Sample code: BS-4 and BS-5 (Tholeiitic)					
Minerals	Modal proportion (%)	Phenocryst maximum grain size (mm)	Phenocryst maximum grain shape	Texture	Rock name
Plagioclase	1-2	0.2mm		Trachytic	Aphyric trachy flow Basaltic andesite
Groundmass of: plagioclase, and opaque minerals	98-99				

Sample code: BS-2and Bs-10 (tholeiitic)					
Minerals	Modal proportion (%)	Phenocryst maximum grain size (mm)	Phenocryst maximum grain shape	Texture	Rock name
Plagioclase	30	0.5mm	Euhedral	porphyritic	Plagphyric basalt
Groundmass of: plagioclase, and opaque minerals	70				

Sample code: BS-9 (Transitional)				
Minerals	Modal proportion (%)	Phenocryst maximum grain size (mm)	Texture	Rock name
Plagioclase	10	Euhedral	Olivine phyric	Olivine phyric Basalt
Olivine	20	Euhedral		
pyroxene	4			
Groundmass of plagioclase, olivine, clinopyroxene, orthopyroxene, and other opaque minerals.	66			

Sample code; BS-11 (tholeiitic)					
Minerals	Modal proportion (%)	Phenocryst maximum grain size (mm)	Phenocryst maximum grain shape	Texture	Rock name
Plagioclase	21%	2mm	Euhedral	porphyritic or Plag phyric	Plag phyric dolerite
Pyroxene	4%				
Groundmass of: plagioclase, pyroxenes and opaque minerals	75%				